

Models of Non-Singular Gravitational Collapse

by

Sonny Campbell (CID: 00891540)

Supervisor: Prof. João Magueijo

Department of Physics
Imperial College London
London SW7 2AZ
United Kingdom

Thesis submitted as part of the requirements for the award of the
MSc in Quantum Fields and Fundamental Forces, Imperial College
London, 2013-2014

Acknowledgements

I would like to thank my supervisor Prof. João Magueijo for his help in deciding on the topic of Planck Stars for my thesis.

I would like to thank Dara McCreary for his help proof-reading and spell checking everything, as well as general article writing advice.

I would like to thank Chris Primo, first for teaching me the meaning of the word conjunction. And then preposition.

A massive thank you to everyone in the QFFF course, who made even the hardest moments great fun, and whom I will never forget.

Finally, thanks to my parents. They have always supported me and encouraged my love of physics, and without them I wouldn't be the physicist I am today.

Contents

1	Introduction: Planck Stars and Asymptotic Freedom	5
2	Dust Models of Gravitational Collapse	10
2.1	Homogeneous Dust Collapse	10
2.1.1	Oppenheimer-Snyder Model	10
2.1.2	Shell Collapse	13
2.1.3	Instability of the Collapse	14
2.1.4	Naked Singularity or Black Hole?	16
2.2	Inhomogeneous Dust Collapse	17
2.2.1	Lematre-Tolman-Bondi Models	17
2.2.2	Singularity Formation	19
2.2.3	Instability of the Collapse	21
2.3	Non-singular Dust Collapse Model	23
2.3.1	Quantum-Corrected Gravitational Collapse	23
2.3.2	Quantum-Corrected Homogeneous Dust Model	25
2.3.3	Apparent Horizon	27
2.3.4	Quantum-Corrected Inhomogeneous Dust Model	29
2.3.5	Apparent Horizon	31
3	Perfect Fluid Models of Gravitational Collapse	33
3.1	Homogeneous Perfect Fluid Collapse	33
3.1.1	Collapsing Matter Clouds	34
3.1.2	Nature of the Singularity	36
3.1.3	Classic Radiation Model	38
3.2	Inhomogeneous Perfect Fluid Collapse	39
3.2.1	Introducing Inhomogeneities	39
3.2.2	Nature of the Singularity	41
3.3	Non-Singular Fluid Collapse	42
3.3.1	Radiating Star Model	42
3.3.2	Quantum-Corrected Homogeneous Radiation Model	46
3.3.3	Apparent Horizon	47
4	Massless Scalar Field Models of Gravitational Collapse	49
4.1	Homogeneous Massless Scalar Field Collapse	53
4.1.1	Classic Scalar Field Model	54
4.2	Inhomogeneous Massless Scalar Field Collapse	55
4.3	Non-Singular Massless Scalar Field Collapse	57
4.3.1	Quantum-Corrected Homogeneous Massless Scalar Field Model	57
4.3.2	Apparent Horizon	59
5	Conclusions	61

List of Figures

1.1	Penrose Diagram of a Star Undergoing Gravitational Collapse . . .	6
2.1	Dust Scale Factor	27
2.2	Dust Apparent Horizon	28
2.3	Quantum Corrected Homogeneous Dust Collapse	29
2.4	Quantum Corrected Inhomogeneous Dust Collapse	32
3.1	A Schematic Diagram of the Radiating Star Process	45
3.2	Radiation Scale Factor	47
3.3	Radiation Apparent Horizon Graph	48
4.1	Massless Scalar Field Scale Factor	58
4.2	Massless Scalar Field Apparent Horizon Graph	59

1 Introduction: Planck Stars and Asymptotic Freedom

When the life of a star is coming to an end, it exhausts its entire fuel supply, the thermal pressure at the center can no longer prevent gravitational collapse, and the star contracts to find a new equilibrium point. Currently, massive stars have no known mechanism to compensate for the gravitational pressure, and this causes the star to collapse all the way to a singularity. When this happens, our standard classical theories break down and predictability of the spacetime is lost, because the singularity prevents information reaching future null infinity. According to the Cosmic Censorship Conjecture, the singularity must be hidden behind an event horizon, and we call this object a black hole. When Hawking radiation is included, the ingoing radiation has negative energy causing the black hole to shrink, until it reaches the central singularity. However this process does not radiate away all the information contained within the black hole [4], leading to issues concerning the unitarity of the theory, and must mean some of it is lost.

In this paper, I will propose some models of gravitational collapse that do not lead to the singularity, therefore restoring unitarity to our spacetime, and altogether avoiding the information paradox. In these cases, the singularity is replaced with a "quantum bounce". Consider a general spherically symmetric metric of the form

$$ds^2 = -F(r)dt^2 + \frac{1}{F(r)}dr^2 + r^2d\Omega^2. \quad (1.1)$$

Trapping horizons, which determine the area from which null geodesics cannot escape, are given by $F(r) = 0$. A surface, with area $4\pi r^2$, is trapped if $F(r) < 0$, and is untrapped if $F(r) > 0$. For an asymptotically flat spacetime, and black hole of mass m ,

$$F(r) \sim 1 - \frac{2m}{r} \text{ as } r \rightarrow \infty, \quad (1.2)$$

while a regular and flat center requires

$$F(r) \sim 1 - \frac{r^2}{l^2} \text{ as } r \rightarrow 0. \quad (1.3)$$

Here l governs the central energy density, assumed positive. For a metric of the form (1.1), with the above conditions, it can be shown [8] the Einstein tensor has a cosmological constant form

$$G \sim -\Lambda g, \text{ where } \Lambda = 3/l^2. \quad (1.4)$$

Hence we have an effective cosmological constant at small distances, governed by l . This behaviour has previously been proposed as the equation of matter at high density, or as an upper limit to the density/curvature, which would be described fully in a more complete theory of quantum gravity. Since l gives the approximate length scale below which such quantum effects would dominate, it had been expected that l would be of the order of the Planck length.

Recently however, it has been proposed that these effects may kick in at scales much larger than the Planck length, and would be instead governed by the scale of the Planck density. According to recent results in Loop Quantum Cosmology, the Friedmann equation that governs $a(t)$, the scale factor of the universe, should be modified as

$$\left(\frac{\dot{a}}{a}\right)^2 = \frac{8\pi G}{3}\rho\left(1 - \frac{\rho}{\rho_{cr}}\right). \quad (1.5)$$

This would indicate that nature enters the quantum gravitational regime around $\rho \sim \rho_P$. Given that $\rho_P \sim m_p/l_P^3$, we can estimate that the volume at which quantum gravitational effects would begin to dominate should be given by

$$V \sim \frac{m}{m_P} l_P^3,$$

and this could happen at scales much larger than that of the Planck length.

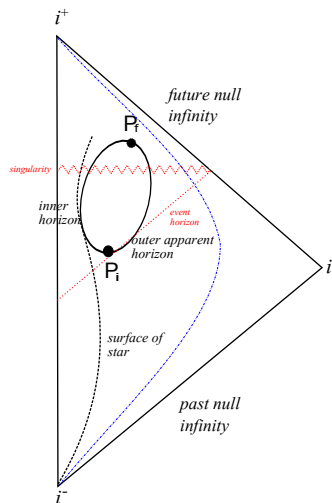


Figure 1.1: **Penrose Diagram of a Star Undergoing Gravitational Collapse**

P_i is the point at which the apparent horizon forms in the process of the collapse, and P_f is the point at which it vanishes again. The red lines indicate what happens in the classical case, as the stellar surface collapses to form a black hole. In the semiclassical case there is no singularity, so no null geodesics are disconnected from future null infinity, and unitarity never even becomes an issue.

According to Rovelli [1], this quantum bounce is due to a quantum gravitational repulsion originating from the Heisenberg uncertainty principle, similar to the "force" that keeps an electron from falling into the center of a nucleus. On the other hand, Bambi et al. [6] proposed that this repulsion is not actually quantum mechanical in nature, but that the bounce follows from the dynamics of the system. In the effective picture, they propose that the bounce comes from the conservation of the energy-momentum tensor, since $\rho_{eff} + p_{eff} < 0$ at the time of the bounce, violating the energy conditions, and is therefore unstable, causing the bounce to

occur. In either case, we will not know until we have a more complete picture of quantum gravity.

We can mimic the quantum gravitational repulsive force by correcting $F(r)$ as

$$F(r) = 1 - \frac{2mr^2}{r^3 + 2l^2m} \approx 1 - \frac{2m}{r} + \frac{4l^2m^2}{r^4}, \quad (1.6)$$

where we have expanded the last part in $1/r$, which gives a regular metric everywhere. This will reduce to a Schwarzschild black hole for $l = 0$, and to a flat spacetime for $m = 0$. Analysis [9] of $F(r)$ gives a critical mass of $m_* = (\frac{3\sqrt{3}}{4})l$ and critical radius $r_* = \sqrt{3}l$. For $r > 0$, if $m < m_*$ then $F(r)$ has no zeros, one double zero at $r = r_*$ if $m = m_*$, and two simple zeros at $r = r_{\pm}$ if $m > m_*$. These three cases describe:

1. A flat spacetime with a regular causal structure.
2. A regular extreme black hole with a degenerate Killing horizon
3. A regular non-extreme black hole with an outer and inner trapping/Killing horizon at $r_+ \approx 2m, r_- \approx l$ for $m \gg m_*$

Hence, black holes with mass $m < m_*$ cannot form. Next we rewrite the metric in terms of advanced time Eddington-Finkelstein coordinates

$$ds^2 = -F(r)dv^2 + 2dvdr + r^2d\Omega^2 \quad (1.7)$$

and allow the mass to depend on the advanced time, $m(v)$. The density, and the transverse and tangential pressures have the same form in these new coordinates, but there is now a radially ingoing energy flux, from the T_v^r component of the Einstein equations, given by

$$G_v^r = \frac{2r^4m'}{(r^3 + 2l^2m)^2}, \quad (1.8)$$

where $m' = dm/dr$. This is a description of pure radiation, which we need to match with an external Vaidya solution. However in these models the center remains totally regular, being protected by the "quantum repulsion" of an effective cosmological constant. The ingoing flux is positive if m is increasing or negative if m is decreasing, but the trapping horizons still occur at $F(r, v) = 0$.

Outgoing Hawking radiation does not enter the equation of motion of the trapping surface, but we model it as in [12] and [13] so that at some $r_0 > 2m_0$ there is negative energy inside that region only, balanced by outgoing radiation outside the boundary. This Hawking radiation will shrink the outer horizon, which we represent in the metric by our time dependence of m . However the inner horizon receives positive energy (since the partner with negative energy in the Hawking pair has positive energy when in-falling), and therefore expands the inner horizon. This process continues until the growing inner horizon meets the outer shrinking horizon, where all the trapped surfaces are released and information inside can escape. A key point in this process is that the inner horizon never reaches the center, so a singularity never forms. Once the trapping horizons reunite, particle production ends.

One inevitable effect of these models is the apparent mass loss of the black hole. This is a result of asymptotic freedom, whose only necessary condition is that gravity becomes very weak at densities approaching the Planck scale. The object should appear as a black hole with time-dependent mass, and this is quite a general prediction. The explicit dynamics of the system will depend on the framework used to describe it, as well as on the physical content such as equation of state, or matter content, but we should see the same general picture.

This seems to me to be a very intuitive idea, much more so at least than the existence of a singularity. Given some of the extremely complex ideas that have been proposed to solve the issues surrounding black holes, we have described a regular spacetime with a simple, flat causal structure. For an observer at infinity the whole process is seen in "slow motion", due to the extreme gravitational time dilation of the system. It would appear as though a black hole existed in the spacetime, due to the strength of the gravity around the collapsing star, but there is never a violation of causality and unitarity is not even an issue.

Section 2 of this paper covers the dust models of gravitational collapse. I will review and combine the latest work in the area to give an overall picture of how a spherically symmetric dust ball would gravitationally collapse in the homogeneous and inhomogeneous cases, and show that the current collapse process is very unstable. The collapse of such an object will only certainly result in a black hole if the object is homogeneous. Under small perturbations from this model it can just as easily form a naked singularity, depending on the initial pressure profile. We will see that a black hole can only result from a very finely tuned collapse, which seems very unlikely for a realistic scenario. However, if the end stage of the process is a naked singularity this contradicts with the Cosmic Censorship Conjecture, pointing to something being fundamentally flawed in our current understanding of the collapse process.

I will then show using assumptions about the density that follow from the above description of Planck stars, we can get a collapse process that halts at a certain density before re-expanding indefinitely. It is a very intuitive idea, and alleviates many of the instability and causality issues that arise from a singular collapse process, as well as avoiding the Cosmic Censorship Conjecture entirely.

In sections 3 and 4, I will similarly review the most current works on the collapse process for perfect fluid and massless scalar field models. In the case of the perfect fluid, inhomogeneities introduced as perturbations from the homogeneous model produce instabilities in the collapse process which are very similar to the dust case. For the inhomogeneous models, any small perturbation will change the outcome of the collapse from a black hole to a naked singularity, again contradicting the Cosmic Censorship Conjecture. The semi-classical "quantum bounce" model is then examined and offers a simple and intuitive solution once more. In section 4 I follow a similar process for examining the massless scalar field model. Using the correspondence of a massless scalar field with that of a stiff fluid, I describe a bounce model for the homogeneous case, and show how it could solve many of the issues that arise through the existence of a singularity.

To date, most of the work on these models has been done for homogeneous matter profiles,

which is the simplest case, but a more realistic inhomogeneous description should give similar results. It would be expected that the density profile is most dense at the center, monotonically decreasing radially outward. In this case, the homogeneous model should still hold for at least the central shell, but the shells at larger radii where the density is lower will have a different dynamical effect on the trapping horizons. What we will show for the bounce models, at least in the case of the dust model, is that since the outer shells bounce before the center, the apparent horizon never actually disappears completely, and that the process is always hidden from observers at infinity.

If these Planck stars do exist, it could have some real astrophysical and cosmological implications. One possibility that has been discussed [1] is that some primordial "black holes" produced in the early universe would have a lifetime of approximately the age of the universe, and could end in our era, which may be detectable. And any model consistent with observations needs to account for the super-massive black hole candidates at the center of galaxies, so trapped surfaces formed during the collapse of these super-massive objects must last for a length of time at least to the order of the age of the universe.

2 Dust Models of Gravitational Collapse

The simplest case of gravitational collapse is the Oppenheimer-Snyder model for marginally bound collapse of a dust sphere. The end product of this process is a black hole in spacetime, as during the collapse process an event horizon forms within the collapsing cloud from which no particles or light rays can escape. The collapsing star enters the horizon and continues until a spacetime singularity is formed, which is hidden from all observers at infinity. The introduction of pressures in dust collapse can stop this from happening, and cause some interesting effects. Classically, we must apply certain conditions to end up with a physically viable model, such as the weak energy condition and the Cosmic Censorship Conjecture, but the occurrence of a simultaneous singularity is closely linked to the homogeneity of the density profile.

The second model I will examine is the generalization of the OS model, known as the Lemaitre-Tolman-Bondi (LTB) model. Inhomogeneities in the pressureless matter profile cause it to lose the simultaneous singularity structure, and different shells become singular at different times. Even more importantly, the behaviour of the horizon changes, so we must determine if a black hole forms or if we are left with a globally or locally naked singularity.

Finally I will look at some non-singular models in which the singularity is avoided by using an effective density, which is the result of work in Loop Quantum Cosmology [2]. The effective density changes the model semi-classically, because we attribute the difference to some unknown quantum effects which kick in when the collapsing star reaches a Planckian density, rather than the usual assumption that effects would kick in at Planckian length. The main difference here is that this can have some interesting effects when the volume of the star is orders of magnitude larger than Planckian volume, so we have a bound on the local curvature as well as on the energy density. The gravitational attraction of the star is replaced by a quantum pressure which causes the star to re-expand, and so a black hole as we know it never actually forms. We call these new objects Planck stars.

2.1 Homogeneous Dust Collapse

2.1.1 Oppenheimer-Snyder Model

The most general spherically symmetric line element describing the collapsing matter cloud as

$$ds^2 = -e^{2\nu(t,r)} dt^2 + e^{2\psi(t,r)} dr^2 + R(t,r)^2 d\Omega^2 \quad (2.1)$$

and the stress-energy tensor for a generic matter sources is given by $T^t_t = -\rho$, $T^r_r = p_r$, $T^\theta_\theta = T^\phi_\phi = p_\theta$. This the most general scenario, without assumptions about the form of matter or equation of state. Using Einstein's equations in natural units, this spacetime can be written as

$$p_r = -\frac{\dot{R}}{R^2 \dot{R}}, \quad (2.2)$$

$$\rho = \frac{F'}{R^2 R'}, \quad (2.3)$$

$$\nu' = 2 \frac{p_\theta - p_r}{\rho + p_r} \frac{R'}{R} - \frac{p'_r}{\rho + p_r}, \quad (2.4)$$

$$\dot{G} = 2 \frac{\nu'}{R'} \dot{R} G, \quad (2.5)$$

$$F = R(1 - G + H), \quad (2.6)$$

where $'$ refers to a derivative with respect to r , and $\dot{}$ refers to a derivative with respect to t . The function $F(r, t)$ is interpreted as the Misner-Sharp mass function, which is proportional to the amount of matter in shell labelled by r at time t . The functions H and G are defined $H = e^{-2\nu(r,a)} \dot{R}^2$ and $G = e^{-2\psi(r,a)} R'^2$. The area radius R is set equal to the comoving radius r at initial time $t_i = 0$, $R(r, 0) = r$, and we introduce an overall scale function $a(r, t)$ such that

$$R(r, t) = r a(r, t) \quad (2.7)$$

So our scale function has the properties $a(t_i, r) = 1$, $a(t_s(r), r) = 0$, and $\dot{a} < 0$, where the time $t = t_s(r)$ corresponds to the shell-focusing singularity at $R = 0$. Using the $a(r, t)$ description has the advantage that it allows us to distinguish between the regular centre of the cloud, the point where the comoving radius $r = 0$, and the genuine singularity where the density and curvature diverge. This is due to the curvature scalars remaining finite at $r = 0$, even though R goes to zero there too. We define all the relevant functions in terms of these new coordinates (r, a) , where any function $X(r, t)$ becomes a function $X(r, a)$ with $X' = X_{,r} + X_{,a} a'$ and $a'(r, t)$ itself is treated as a function of r and a .

We now have five field equations in ρ, ψ, ν, R , and F , and we solve these subject to the weak energy condition and certain regularity conditions for the collapse at the initial spacelike hypersurface $t = t_i$. The evolution of this initial data will determine the final states of the gravitational collapse. There are different classes of solutions based on these initial conditions that will result in either a black hole or a naked singularity.

We now consider a general mass function $F(r, t)$ for the collapsing cloud, which can be written as

$$F(r, t) = r^3 M(r, a) \quad (2.8)$$

where M is a suitably differentiable, regular function with $M > 0$. From the regularity and finiteness of the density profile at the initial $t = t_i$, we require that F goes like r^3 close to the centre. From equations (2.2), (2.3), and (2.7), we see that

$$\rho = \frac{3M + r[M_{,r} + M_{,a} a']}{a^2(a + r a')}, \quad (2.9)$$

$$p_r = -\frac{M_{,a}}{a^2}. \quad (2.10)$$

But in the Oppenheimer-Snyder case we take $p_r = p_\theta = 0$, so from equation (2.2) we have

$$\frac{dF}{dt} = r^3 \frac{dM(r, t)}{dt} = 0,$$

$$\Rightarrow M = M(r).$$

The collapsing cloud can be matched to a Schwarzschild exterior with total mass $2M_T = F(r_b)$ at the boundary r_b . From (2.4) we see that $\nu' = 0$, and we can choose a gauge such that $\nu = 0$. Therefore equations (2.5) and (2.6) imply

$$G = 1 + f(r),$$

$$\dot{R} = \pm \sqrt{\frac{F}{R} + f(r)}, \quad (2.11)$$

where the plus sign describes expansion and the minus sign describes collapse. In general F and f are free parameters of the system which we choose to correspond to physically realistic conditions. The solution can always be matched with a Schwarzschild exterior at the boundary $R_b(t) = R(r_b, t)$.

To integrate equation (2.11), there are three possible cases for the value of f [26]:

1. Hyperbolic region where $f > 0$ which corresponds to an unbound collapse. The particles in the cloud have positive initial velocity in the limit $R \rightarrow \infty$.
2. Flat region where $f = 0$ which corresponds to a marginally bound collapse. The particles in the cloud have zero initial velocity in the limit $R \rightarrow \infty$.
3. Elliptic region where $f < 0$ which corresponds to a bound collapse. The particles in the cloud have negative initial velocity in the limit $R \rightarrow \infty$.

For the purpose of this paper we will be focusing on the marginally bound case, where $f(r) = 0$.

We now have an equation of motion for the Misner-Sharp mass

$$\begin{aligned} \dot{R} &= -\sqrt{\frac{F}{R} + 0}, \\ \Rightarrow \dot{a} &= -\sqrt{\frac{M}{a}}. \end{aligned} \quad (2.12)$$

It is then straightforward to see that

$$a(r, t) = \left(1 - \frac{3}{2}\sqrt{Mt}\right)^{2/3}. \quad (2.13)$$

Since the shells become singular at $a(r, t_s) = 0$, we can see that the singularity is achieved along the curve $t_s = \frac{2}{3\sqrt{M}}$. Since we defined $G = e^{-2\psi(r, a)}(R')^2 \Rightarrow e^{2\psi} = (R')^2/G$, and we know that $a = a(t)$, the metric becomes

$$ds^2 = -dt^2 + a^2(dr^2 + r^2d\Omega^2). \quad (2.14)$$

For the OS dust collapse model, the choice of $M(r) = M_0$ causes the density to be homogeneous. We are left with

$$\rho(t) = \frac{3M_0}{a^3}, \quad (2.15)$$

$$M_0 = a\dot{a}^2, \quad (2.16)$$

$$a(t) = \left(1 - \frac{3}{2}\sqrt{Mt}\right)^{2/3}, \quad (2.17)$$

where all the shells become singular at the same comoving time $t_s = \frac{2}{3\sqrt{M}}$. The apparent horizon curve is given by (2.30)

$$t_{ah} = t_s - \frac{2}{3}r^3M_0, \quad (2.18)$$

and since the apparent horizon forms before the singularity, the collapse process is at all times covered by the horizon, ending in a black hole.

2.1.2 Shell Collapse

We can also invert the function $a(r, t)$ to obtain the time needed by a matter shell of radius r to reach an event with a particular value of t . We start by defining a general and suitably regular function $A(r, a)$ by $A_{,a} = \nu'/R'$. Then integrating equation (2.5)

$$\begin{aligned} \dot{G} &= 2A_{,a}\dot{R}G, \\ &= 2A_{,a}r\dot{a}G, \\ &= 2r\dot{A}G, \\ \Rightarrow G(r, t) &= b(r)e^{2rA}. \end{aligned} \quad (2.19)$$

We interpret the arbitrary function of integration $b(r)$ as related to the velocity of the collapsing shells [16], and write it as $b(r) = 1 + r^2b_0(r)$. Using equation (2.6), we see

$$\begin{aligned} b(r)e^{2rA} - e^{-2\nu}\dot{R}^2 &= 1 - \frac{F}{ra}, \\ \Rightarrow e^{-2\nu}r^2\dot{a}^2 &= \frac{F}{ra} + (be^{2rA} - 1), \\ \Rightarrow \frac{da}{dt} &= e^\nu \sqrt{\frac{F}{r^3a} + \frac{b(r)e^{2rA} - 1}{r^2}}, \\ \Rightarrow t(r, a) &= \int_a^1 \frac{e^{-\nu}d\tilde{a}}{\sqrt{\frac{F}{r^3\tilde{a}} + \frac{b(r)e^{2rA} - 1}{r^2}}}. \end{aligned} \quad (2.20)$$

Taking $h(r, a) = \frac{e^{2rA} - 1}{r^2}$, we can rewrite this as

$$\Rightarrow t(r, a) = \int_a^1 \frac{\sqrt{\tilde{a}} d\tilde{a}}{e^\nu \sqrt{b_0(r) a e^{2rA} + ah(r, \tilde{a}) + M(r, \tilde{a})}}. \quad (2.21)$$

The time taken for shell r to reach the spacetime singularity at $a = 0$ is given by $t_s(r) = t(r, 0)$. Because of our regularity conditions for the functions involved, $t(r, a)$ is in general at least \mathcal{C}^2 everywhere, and is continuous at the center, so we can write it as

$$t(r, a) = t(0, a) + r\chi(a) + O(r^2). \quad (2.22)$$

When $t(r, a)$ is differentiable, we Taylor expand near $r = 0$, and the above integral is evaluated at $r = 0$ where

$$\chi(a) = \frac{dt}{dr} = -\frac{1}{2} \int_a^1 \frac{\sqrt{\tilde{a}} B_1(0, \tilde{a})}{B(0, \tilde{a})^{\frac{3}{2}}} d\tilde{a}, \quad (2.23)$$

with

$$\sqrt{B(r, a)} = e^\nu \sqrt{b_0(r) a e^{2rA} + ah(r, a) + M(r, a)}, \quad (2.24)$$

$$B_1(r, a) = B_{,r}(r, a). \quad (2.25)$$

We will show that the quantity $\chi(0)$ is very important in determining the end stage of the gravitational collapse process. The time taken for the shell r in a close neighbourhood of the center to collapse to the singularity will take $t_s(r) = t_s(0) + r\chi(0) + O(r^2)$, and this means the singularity curve should have a well defined tangent at the center. To ensure regularity of the initial data at the center of the cloud, the metric function ν cannot have constant or linear terms in r close to the center. We then take

$$\nu(r, a) = r^2 g(r, a), \quad (2.26)$$

where $g(r, a)$ is at least a C^1 function of r for $r = 0$ and at least a C^2 function for $r > 0$. It can be written near $r = 0$ as

$$g(r, a) = g_0(a) + g_1(a)r + g_2(a)r^2 + \dots \quad (2.27)$$

2.1.3 Instability of the Collapse

To look at the effect of pressure perturbations in the OS collapse model, we need to relax one of the conditions which we applied. We have seen that the dust model ends in a simultaneous singularity, a black hole, but if the outcome was not a black hole, we cannot have a simultaneous singularity. We relax the condition applied to the scaling function a , giving that $a = a(r, t)$, instead of $a = a(t)$ only. This allowance for small pressure perturbations amounts to perturbations of ν from equation (2.4), permitting it to be non-zero.

Close to the center of the cloud, where $r \rightarrow 0$, we have $R' = a + ra' \rightarrow a$. This gives us $A_{,a} = \nu'/a$, and this small limit $G(r, t) = b(r)e^{2\nu(r,t)}$. We still have $p_r = 0$ as $\dot{F} = 0$, while the tangential pressure has the form [25]

$$p_\theta = \frac{3M_0g_0r^2}{aR'^2} + \frac{9M_0g_1r^3}{2aR'^2} + \dots \quad (2.28)$$

The coefficient χ in $t_s(r)$, the time curve of the singularity, is now

$$\chi(0) = - \int_0^1 \frac{a^{3/2}g_1(a)da}{(M_0 + ab + 2ag_0(a))^{3/2}}. \quad (2.29)$$

This quantity governs the behaviour of the singularity curve, whether it is increasing or decreasing away from the center. It is the system's initial data, such as the density/stress profiles, collapsing shell velocity, and the dynamical evolution, that determine the value of $\chi(0)$. It is also responsible for the apparent horizon and trapped surface formation, which will allow us to check whether the singularity is naked, locally or globally, or whether it is covered by a black hole.

The condition for the formation of trapped surfaces requires that the $R(r, t) = \text{const.}$ surface is null. So we require $g^{\mu\nu}(\partial_\mu R)(\partial_\nu R) = 0$. For the metric (1), this means

$$\begin{aligned} -e^{-2\nu}\dot{R}^2 + e^{2\psi}R'^2 &= 0, \\ \Rightarrow G - H &= 0. \end{aligned}$$

From the definition (2.6) of the Misner-Sharp mass, we can write the trapped surface formation condition as

$$\frac{F}{R} = 1, \quad (2.30)$$

and the apparent horizon curve is given by

$$r_{ah}^2(t) = \frac{a_{ah}}{M_0}. \quad (2.31)$$

Inverting this equation gives $a_{ah} = a(r_{ah}(t), t)$, which in turn will give us the time curve $t_{ah}(r)$. We can determine whether the singularity is visible at infinity by the nature of this apparent horizon curve, given by

$$t_{ah}(r) = t_s(r) - \int_0^{a_{ah}} \frac{e^{-\nu} da}{\sqrt{\frac{M_0}{a} + \frac{be^{2\nu}-1}{r^2}}}, \quad (2.32)$$

and near to $r = 0$ this becomes

$$t_{ah}(r) = t_s(0) + \chi(0)r + O(r^2). \quad (2.33)$$

We can now check how the pressure perturbations affect the time of the apparent horizon formation, and this will allow us to determine whether a black hole forms or we have a naked singularity.

2.1.4 Naked Singularity or Black Hole?

The end state of a gravitationally collapsing object is typically considered a naked singularity when a comoving observer at fixed r doesn't meet any trapped surfaces until the time that the singularity forms. Hence, for a black hole to form, the trapped surfaces must form before the singularity

$$\Rightarrow t_{ah}(r) \leq t_s(0) \text{ for } r > 0, \text{ near } r = 0, \quad (2.34)$$

Clearly for all functions $g_1(a)$ such that $\chi(0) > 0$, this condition is violated and the apparent horizon therefore must form after the singularity. The apparent horizon curve then begins at $r = 0$ and $t = t_s(0)$, and increases with increasing r moving into the future

$$\Rightarrow t_{ah} > t_s(0) \text{ for } r > 0.$$

This means that null geodesics can originate at the singularity as seen from infinity, making it visible to external observers. Therefore we would have a naked singularity.

Clearly $g_1(a)$ is the term from the tangential pressure perturbations p_θ which determines whether we have a naked singularity forming, or a black hole. We can choose it to be arbitrarily small, but even the tiniest change in inner pressures will change the outcome of the collapse dramatically. This gives us a very interesting insight into the nature of the Cosmic Censorship Conjecture, in that gravitational collapse would have to be very precise and fine-tuned to prevent a naked singularity and result in a black hole end-state.

2.2 Inhomogeneous Dust Collapse

From the discussion on the OS collapse model, we see it is characterised by two main features, the occurrence of a simultaneous singularity and the appearance of trapped surfaces before the singularity, which are both closely linked to the homogeneity of the initial density profile. We will now examine a slightly more general matter profile, where a simultaneous singularity is a feature of only very few collapse scenarios.

The simplest generalisation of the OS model is the Lemaitre-Tolman-Bondi(LTB) inhomogeneous dust collapse. Inhomogeneities in the pressureless matter profile cause the collapse to lose its simultaneous singularity structure, as each shell becomes singular at a different time. Another consequence of the inhomogeneities is that the apparent horizon behaviour is changed, resulting in the possibility for the singularity at the center becoming locally or globally naked. Some matter profiles still cause the horizon to form before the formation of the singularity, while others develop trapped surfaces at the time of formation of the singularity, leaving open the possibility for geodesics to escape from the high-density cloud center. These models are of course only simple mathematical models that do not describe a realistic star, however they let us examine the important features that determine the end state of a gravitational collapse.

This section will characterize the process of black hole formation with some physically reasonable requirements, such as positive and radially decreasing density, and the absence of shell crossing singularities. We will show that once these requirements are imposed, the only models which develop a black hole have a simultaneous singularity, and all other allowed scenarios having non-constant singularity curve develop a locally naked singularity.

2.2.1 Lemaitre-Tolman-Bondi Models

The LTB metric describing inhomogeneous dust in comoving coordinates is given by

$$ds^2 = -dt^2 + \frac{(R')^2}{G} dr^2 + R^2 d\Omega^2, \quad (2.35)$$

where again $R = R(r, t)$ and $f = f(r)$. Requiring a Lorentzian metric imposes a condition on the energy function $f(r)$ such that $f(r) \geq -1$. Again, from equation (2.6) we have

$$F = R(\dot{R}^2 - f(r)), \quad (2.36)$$

which gives us $F = F(r)$, the MS-mass, describing the amount of matter enclosed in any shell labelled r . And once again

$$\Rightarrow \dot{R} = \pm \sqrt{\frac{F}{R} + f}. \quad (2.37)$$

The integration of (2.37) gives us

$$t(r, R) = -\frac{2}{3\sqrt{F}}(R)^{3/2} + k(r), \quad (2.38)$$

$$\Rightarrow R(r, t) = \left(\frac{3}{2} \sqrt{F}(k(r) - t) \right)^{2/3}, \quad (2.39)$$

where $k(r)$ is some integration function that is determined from the initial conditions.

In general, given any curve $R_\gamma(r)$ we will have some $t_\gamma(r) = t(r, R_\gamma(r))$. The curves which are most relevant to solutions of equation (2.37) in gravitational collapse are:

1. $R_s(r) = 0$, the singularity curve, $\Rightarrow t_s(r) = t(r, 0)$ and $t'_s = (\frac{\partial t}{\partial r})_{R=0}$. This gives us the time at which shell r becomes singular. It indicates a strong curvature singularity along the curve, where physical quantities such as the energy density ρ diverge.
2. $R_{ah}(r) = F(r)$, the apparent horizon, $\Rightarrow t_{ah}(r) = t(r, F(r))$ and $t'_{ah} = (\frac{\partial t}{\partial r} + \frac{\partial t}{\partial R} F')_{R=F}$. This gives us the time at which shell r becomes trapped behind an apparent horizon. The apparent horizon curve is the boundary of the region where trapped surfaces form, given by the condition $g^{\mu\nu} \partial R_\mu \partial R_\nu = 0$.
3. $R'_{sc}(r) = 0$, the shell crossing singularity, $\Rightarrow t_{sc}$ is given by $R'(r, t_{sc}(r)) = 0$. This gives the time at which shell r intersects another shell. We interpret this as a breakdown of the coordinate system. The singularity is seen in equation (2.3), but is a weak curvature singularity that can be removed by a suitable change of coords.

We now apply regularity conditions to our equations to make them physically reasonable. Regularity of ρ at $r = 0, t_i = 0$ implies

$$\begin{aligned} F(r) &= r^3 M(r), \\ f(r) &= r^2 b(r). \end{aligned}$$

Once again using gauge freedom we set $R(r, t) = ra(r, t)$ such that $a(r, 0) = 1$. Then we can rewrite equation (2.37) as

$$\dot{a} = -\sqrt{\frac{M}{a} + b}, \quad (2.40)$$

and a further condition for collapse is given by $b + M \geq 0$.

The energy density is given by equation (2.3)

$$\rho = \frac{F'}{R^2 R'},$$

and for the model to be physically reasonable we require $\rho \geq 0$, satisfying the weak energy condition, and radially non-increasing outwards. Condition 1 implies $F' \geq 0$ and $R' > 0$. The case where $F' < 0$ and $R' < 0$ is not allowed because it would imply $M < 0$ around the center. $F' > 0 \Rightarrow 3M > -rM' \Rightarrow M(0) > 0$. $R' > 0$ means we avoid shell-crossing singularities.

The second physicality condition is that the energy density be a non-decreasing function of r , giving $\rho' \geq 0$,

$$\Rightarrow F'' \leq F' \left(\frac{2R'}{R} + \frac{R''}{R'} \right). \quad (2.41)$$

Choosing the energy density so that it can be expanded as a power series near $r = 0$ [26]

$$\rho = \rho_0(t) + \rho_1(t)r + O(r^2), \quad (2.42)$$

with $\rho_0(t) = 3M_0/a(o, t)^3$, and $\rho_1(t) = 4M'(0)/a(0, t)^3 - 12M_0a'(0, t)/a(0, t)^4$. Initially, when $a = 1, a' = 0$, we have $\rho_0(0) = 3M_0$ and $\rho_1(0) = 4M'(0)$, so having $\rho' \leq 0 \Rightarrow M'(0) \leq 0$. In most astrophysical models we only have even terms in r appearing in the expansion, so this requires that $M'(0, t) = 0$, implying the absence cusps at center for energy density. Instead we must have $M''(0) \leq 0$.

Integrating equation (2.40) in the flat ($b = 0$) region, we find

$$t(r, a) = -\frac{2a^{3/2}}{3\sqrt{M}} + k(r) \quad (2.43)$$

and when we impose the initial conditions $t_i = 0, R(r, t_i) = r$

$$\Rightarrow k(r) = \frac{2r^{2/3}}{3\sqrt{F}} = \frac{2}{3\sqrt{M}} = t_s(r), \quad (2.44)$$

$$t(r, a) = t_s(r) - \frac{2a^{3/2}}{3\sqrt{M}}. \quad (2.45)$$

where $t_s(r) = t(r, 0)$ is the singularity curve.

2.2.2 Singularity Formation

The Kretschmann scalar, $R^{abcd}R_{abcd}$, for the LTB metric is [26]

$$K = \frac{12F^2}{R^6} + \frac{8FF'}{R^5R'} + \frac{3F'^2}{R^4R'^2}, \quad (2.46)$$

and we can see there are singularities forming when $R = 0$ or $R' = 0$. We have already established that $R' = 0$ is a shell crossing singularity, and is typically 'weak', since it is due to coordinate breakdown and can be removed by a change of coordinates. The condition for avoidance of shell crossing is $R' > 0$, so once we solve the equation of motion for $t(r, a)$ we can evaluate $R' = -\frac{\partial t}{\partial r}\dot{R}$, to find further conditions. Requiring no shell crossing implies $\frac{\partial t}{\partial r} > 0$, since $\dot{R} < 0$ for collapse models.

For the marginally bound case [19]:

$$\begin{aligned} R' = -\frac{\partial t}{\partial r}\dot{R} &= -\frac{\partial}{\partial r} \left(t_s(r) - \frac{2a^{3/2}}{3\sqrt{M}} \right) \left(-\sqrt{\frac{F}{R}} \right), \\ \Rightarrow 2R' &= \frac{\sqrt{r}}{\sqrt{R}} + \frac{1}{3} \frac{R^{3/2} - r^{3/2}}{\sqrt{R}} \frac{F'}{F}. \end{aligned} \quad (2.47)$$

The no shell crossing condition gives

$$3F > F' \left(r - \frac{R^{3/2}}{r^{1/2}} \right) \Leftrightarrow M'(1 - a^{3/2}) < 0, \quad (2.48)$$

and since $a \in [0, 1]$ we must have that $M' < 0$. We can find the shell crossing curve by setting $R' = 0$, and we do this in equation (2.47) to get

$$t_{sc}(r) = \frac{2\sqrt{M}}{3M + rM'}, \quad (2.49)$$

and from this we can see that $M = const \Rightarrow t_{sc} = t_s$, and $M' < 0 \Rightarrow t_{sc} \geq t_s$, where they are only equal at $r = 0$, and no shell crossings occur.

On the other hand, applying the condition that the singularity curve is non-increasing, which is the condition for the formation of a black hole, the singularity curve given by (2.44) indicates

$$\begin{aligned} t'_s &= \frac{\sqrt{r}}{\sqrt{F}} \left(1 - \frac{F'r}{3F} \right) \leq 0, \\ &\Rightarrow 3F \leq F'r, \\ &\Rightarrow M' \geq 0. \end{aligned} \quad (2.50)$$

Clearly we have a contradiction, telling us that black hole formation and no shell crossings are incompatible conditions for marginally bound LTB collapse. The only exception is the simultaneous collapse case, where $t_s(r) = t_0$. This also means that, again excluding the simultaneous collapse case, having positive energy density and radially non-increasing outward is compatible with no shell crossings, but not with the black hole formation process. In my opinion, what we're seeing is that some very reasonable physical conditions contradict with formation of a black hole throughout the collapse process in this model, implying that the black hole formation process violates some basic physical principles.

The general conditions for avoidance of shell-crossings were given by Hellaby and Lake [18], and assuming $F > 0, F' > 0$ in the marginally bound case, we have that $t'_s \geq 0$. The apparent horizon curve is given by $R_{ah} = F(r)$, which implies

$$t_{ah}(r) = t_s(r) - \frac{2}{3}F(r), \quad (2.51)$$

and $t_{ah}(r) \rightarrow t_s(0)$ as $r \rightarrow 0$. It was shown by Goswami and Joshi [44] that, generally, an increasing apparent horizon is a sufficient condition for the locally visibility of the singularity. So $t'_s > 0$ near the singularity implies t_{ah} is increasing near $r = 0$, and the singularity will be locally naked. From this we see that the shell-crossing singularity condition means the only process which ends with a black hole, where the singularity curve is at all times trapped, is the case of the simultaneous singularity $t_s = t_0$. Therefore, under our physically reasonable conditions, the only process where an inhomogeneous dust model can collapse gravitationally to a black hole is the simultaneous collapse model. All other physically valid processes which end as a singularity will be locally or globally naked, and violate the Cosmic Censorship

Conjecture. Whether the singularity is globally or locally naked will depend on the initial matter configuration, but regardless the Cosmic Censorship Conjecture is still violated.

The condition for simultaneous collapse is that all the shells fall into the central singularity at the same comoving time $t_s(r) = t_0$, which is only satisfied if $M = M_0$, a constant. This corresponds to the model of OS collapse discussed before. We can also use the no shell-crossing condition $t'_s > 0$, giving

$$t'_s(r) = -\frac{M'}{3M^{3/2}} > 0, \quad (2.52)$$

which is satisfied when $M' < 0$, agreeing with the positive and decreasing energy density condition and the formation of a locally naked singularity.

2.2.3 Instability of the Collapse

I will now demonstrate how arbitrarily small pressure perturbations of the LTB model can dramatically effect the endstate of collapse, where 'small' means the pressure is much smaller than the energy density at all times. The spacetime singularity curve, corresponding to $a(r, t_s) = 0$, is written in a neighborhood of the center as

$$t_s(r) = t_0 + \chi_1(0)r + \chi_2(0)r^2 + o(r^3), \quad (2.53)$$

from the formalism described in [44], and by expanding $b(r) = b_0 + b_1r + b_2r^2..$ we find

$$\begin{aligned} \frac{\partial t}{\partial r}_{r=0} &= \chi_1(0) = -\frac{1}{2} \int_0^1 \frac{M_1 + b_1a}{(M_0 + b_0a)^{3/2}} da, \\ \frac{\partial^2 t}{\partial r^2}_{r=0} &= \chi_2(0) = \frac{3}{8} \int_0^1 \frac{(M_1 + b_1a)^2}{(M_0 + b_0a)^{5/2}} da - \frac{1}{2} \int_0^1 \frac{M_2 + b_2a}{(M_0 + b_0a)^{3/2}} da. \end{aligned}$$

The overall behaviour of the collapsing cloud is determined by $M(r, t)$, the evolution $a(r, t)$, and the initial velocity profile $b(r)$. Our LTB model has $M = M(r)$, $b_0(r) = 0$. To perturb the LTB model, we require $a = a(r, t)$, rather than just $a(t)$, and therefore the simultaneous collapse, which is required for black hole formation, doesn't happen. As seen previously, this allowance for pressure perturbations corresponds to perturbations of ν in equation (2.4), so it can be non-zero.

Taking the matter profile to be

$$M = M_0 + M_2(a)r^2,$$

where M_0 is a constant, we immediately see that $M_2 = C$ reduces the model to inhomogeneous dust, and $M_2 = 0$ gives us the OS collapse model. Hence, in this model $\chi_1 = 0$ and

$$\chi_2(0) = -\frac{1}{2} \int_0^1 \frac{M_2\sqrt{a}}{M_0^{3/2}} da = -\frac{M_2}{3M_0^{3/2}}, \quad (2.54)$$

$$\Rightarrow t_s(r) = t_0 + \chi_2(0)r^2 + O(r^3) \quad (2.55)$$

We can see that $t_s \geq t_0$ for all $M_2 < 0$, and this will end the process in a naked singularity. If we now add in a small tangential pressure near the center, then similar to the homogeneous case we get a pressure of the form [22]

$$p_\theta = \frac{r^2}{aR^2} \left(3M_0g_0 + \frac{9}{2}M_0g_1 + \dots \right) \quad (2.56)$$

For the marginally bound case, we always have $\chi_1 = 0$, but the pressure p_θ will have an effect on ν via equation (4), so we must add this back into our calculation of χ_2 . As in equation (2.21), taking $h(r, a) = h_0(a) + h_1(a)r + \dots = \frac{e^{2rA}-1}{r^2}$ [22], we get

$$\chi_2(0) = -\frac{1}{2} \int_0^1 \frac{\frac{M_2}{a} + 2h_2 + 2h_0^2 + 2g_0(\frac{M_0}{a} + 2a_0)}{(\frac{M_0}{a} + 2a_0)^{3/2}} da \quad (2.57)$$

Now we can see, in a similar fashion to the homogeneous dust model case, that if g_0 is chosen in such a way that χ_2 is positive, the final stage of the gravitational collapse will be a naked singularity, rather than a black hole. We have therefore constructed a class of models of small tangential pressure perturbations of the LTB model collapse that drastically change the final outcome of the collapse process with the introduction of small pressures.

Once again we have a model of collapse, on which we have placed some reasonable physicality and reality conditions, that requires some very fine tuning to actually collapse to a black hole. The far more likely end product of the collapse would be a naked singularity, but this is in violation of the Cosmic Censorship Conjecture. The main question I focus on in this thesis is how do we resolve this contradiction?

2.3 Non-singular Dust Collapse Model

2.3.1 Quantum-Corrected Gravitational Collapse

The most important feature about the onset of quantum-gravitational effects in these models comes from a recent idea in loop quantum cosmology [2]. The Friedmann equation that governs the dynamics of $a(t)$, the scale factor, is modified by quantum gravitational effects as

$$\left(\frac{\dot{a}}{a}\right)^2 = \frac{8\pi G}{3}\rho\left(1 - \frac{\rho}{\rho_{cr}}\right). \quad (2.58)$$

The quantum correction term is determined by the ration of ρ to a density of Planckian scale

$$\rho \sim m_p/l_p^3 \sim c^5(\hbar G^2),$$

where m_p and l_p are the Planck mass and Planck length. This indicates that rather than at a Planckian length scale, as is usually assumed, it is a Planckian density scale where matter enters the quantum gravitational regime. This may happen at scales much larger than the Planck length scale, resulting in a gravitationally collapsing object bounces back to an expanding one, thereby avoiding the singularity end-state. We attribute the bounce to yet undetermined quantum gravitational forces acting on the collapsing matter once it reaches this density, which force the object to start expanding again. When the bounce occurs, the volume of the object is of order

$$V \sim \frac{m}{m_p} l_p^3,$$

where m is the mass of the object. This would imply that the bounce can happen long before the object can collapse to the singularity. If this is the case, we would have one extra phase in the life of a collapsing star, where the extreme gravitational attraction is balanced by an extreme internal quantum pressure. A star in this stage of its life is called a "Planck Star".

What would this process look like from a far away observer? It turns out the life of a Planck star is extremely long as measured by an observer at infinity, because it is determined by the Hawking evaporation time of the black hole in which it is hidden. The extreme gravitational time dilation and the apparent horizon formation would cause a distant observer to see something with many of the properties of a black hole, however, if an observer was sitting on the surface of the star, this collapse/expand process would be extremely short, of the order of time taken for light to cross the radius of the star. The proper lifetime of a Planck star is essentially an extremely quick bounce.

In what follows, we rewrite Einstein's equations as dust + corrections, where ρ_{cr} indicates the scale at which the corrections become relevant. For the corrections to become important at high densities, we write [24]

$$\rho_{corr} = \alpha_1 \rho^2 + \alpha_2 \rho^3 + O(\rho^4), \quad (2.59)$$

$$\Rightarrow \rho_{eff} = \rho + \rho_{corr}, \quad (2.60)$$

where the parameters $\alpha_i(\rho_{cr})$ determine the scale of the corrections and would be determined from the quantum theory. We then take

$$T_{\mu\nu} = T_{\mu\nu}^{class} + T_{\mu\nu}^{corr}.$$

To study how this effective theory with quantum effects included affects the singularity formation, we assume that at first order the corrections are of the form on equation (2.58). We will then consider an effective theory where the corrections to the energy density take the form

$$\rho_{eff} = \rho \left(1 - \frac{\rho}{\rho_{cr}} \right)^\gamma, \gamma \geq 1, \quad (2.61)$$

and we will examine the case where $\gamma = 1$. This is because for $\gamma > 1$, the value of the scale factor $a \rightarrow a_{cr}$ only as $t \rightarrow \infty$. This will be explained in more detail later, but amounts to the process taking an infinite amount of time. The $\gamma = 1$ case corresponds to setting $\alpha_1 = -1/\rho_{cr}$ and $\alpha_i = 0$ for $i > 1$. In the weak field limit with low densities, the effective density approaches the classical density.

2.3.2 Quantum-Corrected Homogeneous Dust Model

Reminding ourselves of the scale function a , in equations (2.15) and (2.16), from the first model

$$\begin{aligned}\rho(t) &= \frac{3M_0}{a^3}, \\ M_0 &= a\dot{a}^2,\end{aligned}$$

and replacing ρ with ρ_{eff} from equation (2.58), we find

$$M_0 = \frac{a^3}{3}(\rho + \alpha_1\rho^2 + \dots) \quad (2.62)$$

$$\Rightarrow a\dot{a}^2 = \frac{a^3}{3}(\rho + \alpha_1\rho^2 + \dots) \quad (2.63)$$

$$\Rightarrow \dot{a}^2 = \frac{M_0}{a} + \alpha_1\frac{3M_0^2}{a^4} + \dots \quad (2.64)$$

Now, considering an effective density of the form (2.61), and integrating, we can solve for ρ, p and M in the effective theory by replacing them with the corresponding effective quantities

$$\rho_{eff} = \frac{3M_{eff}}{a^3}. \quad (2.65)$$

$M_{eff}(t)$ is the effective Misner-Sharp mass, and now depends on t . This will induce an effective pressure p_{eff} in an otherwise pressureless dust.

$$3\frac{\dot{a}^2}{a^2} = \rho\left(1 - \frac{\rho}{\rho_{cr}}\right)^\gamma, \quad (2.66)$$

$$\dot{a}^2 = \frac{M_0}{a}\left(1 - \frac{a_{cr}^3}{a^3}\right)^\gamma, \quad (2.67)$$

$$\dot{a}^2 = \frac{M_0}{a^{3\gamma+1}}(a^3 - a_{cr}^3)^\gamma, \quad (2.68)$$

with $\rho_{cr} = \frac{3M_0}{a_{cr}^3}$. We now have a differential equation for the scale function $a(t)$.

Solving this equation with the initial condition $a(0) = 1$ and $\gamma = 1$ gives

$$\frac{da}{dt} = \sqrt{M_0}\left(\frac{a^3 - a_{cr}^3}{a^4}\right)^{1/2}, \quad (2.69)$$

$$\Rightarrow t(a) = \frac{2}{3\sqrt{M_0}}(\sqrt{1 - a_{cr}^3} - \sqrt{a^3 - a_{cr}^3}). \quad (2.70)$$

Because of the effective energy density, the new dynamics cause the system to have an effective pressure given by equation (2.2):

$$p_{eff}(t) = -\frac{\dot{M}_{eff}}{a^2\dot{a}}. \quad (2.71)$$

This effective pressure comes from the quantum correction terms, and is homogeneous as well.

$$M_{eff} = M_0 \left(1 - \frac{\rho}{\rho_{cr}} \right), \quad (2.72)$$

$$\Rightarrow p_{eff} = -\frac{\rho^2}{\rho_{cr}}. \quad (2.73)$$

The effective pressure is always negative and approaches $p = -\rho$ as $\rho \rightarrow \rho_{cr}$, and it is this negative pressure that causes the bounce as it reaches the quantum level.

Rearranging (2.70), the scale function $a(t)$ has the form

$$a(t) = \left[a_{cr}^3 + \left(\sqrt{1 - a_{cr}^3} - \frac{3\sqrt{M_0}}{2} t \right)^2 \right]^{1/3}, \quad (2.74)$$

and reaches the minimum value a_{cr} in finite time, as shown in figure (2.1)

$$t(a_{cr}) = t_{cr} = \frac{2\sqrt{1 - a_{cr}^3}}{3\sqrt{M_0}} < t_s. \quad (2.75)$$

At this time, $\rho = \rho_{cr}$, so $\rho_{eff} = 0$ and begins to increase for $t > t_{cr}$. We also find

$$\ddot{a}(t) = -\frac{3M_0}{2} \left[\frac{4}{3} a^{-5} \left(\sqrt{1 - a_{cr}^3} - \frac{3\sqrt{M_0}}{2} t \right)^2 + a^{-2} \right], \quad (2.76)$$

which at t_{cr} reaches

$$\Rightarrow \ddot{a}(t_{cr}) = -\frac{3M_0}{2} a_{cr}^{-2}. \quad (2.77)$$

Contrary to the classical dust case where ρ diverges at $t_s = 2/3\sqrt{M_0}$, the density now tends to a maximum ρ_{cr} as $t \rightarrow t_{cr}$ and then decreases. The velocity of the collapsing shells $\dot{a} \rightarrow 0$ as $t \rightarrow t_{cr}$. Since a never goes to zero, the value of the Kretschmann scalar [24]

$$R^{abcd}R_{abcd} = 12 \frac{\ddot{a}^2 a^2 + \dot{a}^4}{a^4} \quad (2.78)$$

never diverges. We also remove the possibility for shell crossing singularities because we have a system that is equivalent to a homogeneous perfect fluid, with $R(r, t) = ra(t)$, and the scale function $a(t)$ is everywhere positive, therefore the spacetime is everywhere regular.

From equation (2.71) we see that M_{eff} decreases, becoming zero when $t = t_{cr}$. We can match the exterior spacetime with the Vaidya solution for outgoing radiation.

We can also clearly see that since $M(t_{cr}) = \rho(t_{cr}) = 0$, the spacetime must be flat at this stage. This is because in our model, as $\rho \rightarrow \rho_{cr}$, the gravity becomes weaker and weaker until it is finally turned off. After this point the model describes an expanding cloud with $\dot{a} > 0$. If this is true, there may be some astronomical phenomena that could be explained by this process. It is plausible that this process could be the cause of some of the high-energy phenomena observed today.

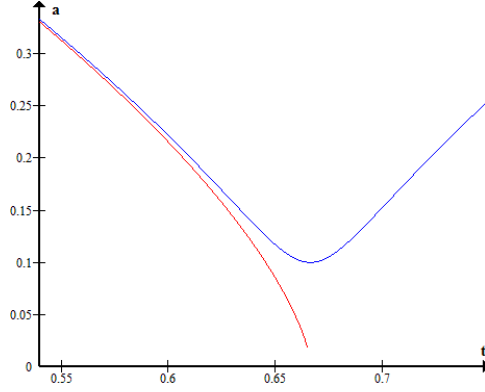


Figure 2.1: **Dust Scale Factor**

In this graph the red line indicates the scale factor $a(t)$ in the classic case, whereas the blue line represents the quantum corrected model. Initially, in the weak-field regime, the semi-classical model behaves in a similar way to the classical case, however once we get close to t_{cr} the quantum effects become important, and the scale factor diverges from the classical case. We have taken $M_0 = 1$ and $\rho_{cr} = 3000$.

2.3.3 Apparent Horizon

The apparent horizon is again defined as the curve $t_{ah}(r)$ for which $a(r, t_{ah}) = r^2 M_{eff}(r, t_{ah}(r))$. For the classical OS model, from equation (2.18) we find it to be given as

$$t_{ah} = t_s - \frac{2}{3} r^3 M_0.$$

For the semi-classical model

$$a = r^2 M_0 \left(1 - \frac{\rho}{\rho_{cr}} \right) \quad (2.79)$$

$$\Rightarrow r_{ah} = \frac{a^2}{\sqrt{M_0(a^3 - a_{cr}^3)}} \quad (2.80)$$

The curve r_{ah} has a minimum at

$$\frac{dr}{dt} = 0 \Rightarrow a^3 = 4a_{cr}^3, \quad (2.81)$$

$$\Rightarrow t_{min} = \frac{2}{3\sqrt{M_0}} (\sqrt{1 - a_{cr}^3} - \sqrt{3a_{cr}^3}). \quad (2.82)$$

This implies there must also exist a minimum radius

$$r_{min} = r_{ah}(t_{min}) = 2^{4/3} \sqrt{\frac{a_{cr}}{3M_0}}. \quad (2.83)$$

This is the limiting radius for which, if $r_b < r_{min}$, no trapped surface can form at any stage of the collapse. Hence, this gives us a threshold mass below which the collapsing matter

cloud can always be seen by an observer at infinity. From the boundary condition for the collapse, $2M_T = r_b^3 M_0$, M_T being the total mass, we find this threshold mass is

$$M_{min} = 8\sqrt{\frac{a_{cr}^3}{27M_0}}. \quad (2.84)$$

After t_{cr} the cloud starts to expand again, and another trapped region forms. This is due to the gravitational strength growing once the system leaves asymptotic freedom. Since the object is expanding now the density starts to decrease, and once it becomes too low the apparent horizon disappears forever.

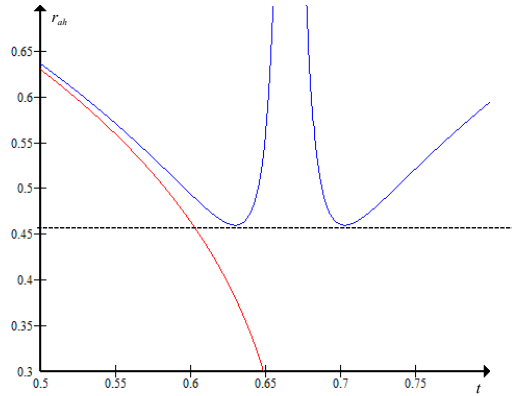


Figure 2.2: **Dust Apparent Horizon**

This is a graph of the apparent horizon curve $r_{ah}(t)$ for the classical model (red line) and semiclassical model (blue line). We can clearly see that as $t \rightarrow t_{cr}$, $r_{ah} \rightarrow \infty$, so the process becomes visible to an observer an infinity for a brief period of time.

The whole process would look something like figure (2.3), where we can clearly see that no geodesics are disconnected from future null infinity.

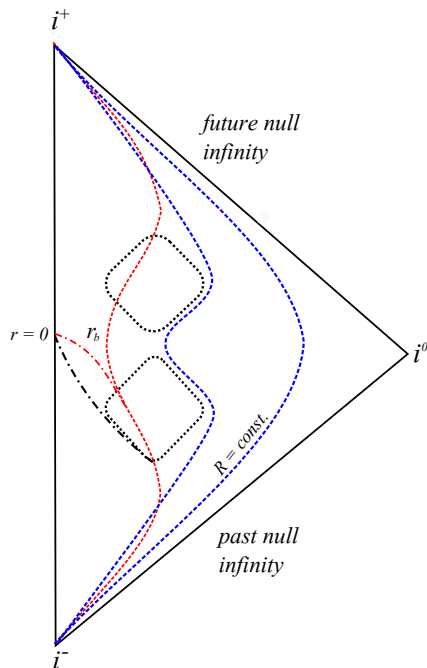


Figure 2.3: **Quantum Corrected Homogeneous Dust Collapse**

Penrose diagram for the semiclassical homogeneous dust collapse model discussed above. The black lines correspond to the trapped surface of the collapsing object. The red dotted line is the boundary curve of the collapsing object. The dashed-dotted black and red lines correspond to the classical collapse case. At some point after the collapse starts the quantum effects kick in, and the semiclassical solution departs from the classical singularity formation.

2.3.4 Quantum-Corrected Inhomogeneous Dust Model

We now examine a model in which inhomogeneities are introduced, but that recovers the classical case once ρ_{cr} goes to zero, and recovers the homogeneous case once the density perturbations go to zero. We will examine the structure at the center of the cloud, near $r = 0$, by Taylor expanding certain quantities. By expanding, we reduce the system of five coupled partial differential equations (2.2) - (2.6) to two coupled ordinary differential equations. Using equation (2.3) in

$$\rho_{eff} = \rho \left(1 - \frac{\rho}{\rho_{cr}} \right), \quad (2.85)$$

we find that the effective mass function and scale function can be expanded in powers of r as [27]

$$a(r, t) = a_0(t) + r^2 a_2(t) + \dots, \quad (2.86)$$

$$M_{eff} = M_{0,eff} + r^2 M_{2,eff} + \dots, \quad (2.87)$$

where

$$M_{0,eff} = M_0 \left(1 - \frac{3M_0}{a_0^3 \rho_{cr}} \right), \quad (2.88)$$

$$M_{2,eff} = M_2 \left(1 - 6 \frac{M_0}{a_0^3 \rho_{cr}} \right) + 9 \frac{M_0^2 a_2}{\rho_{cr} a_0^4}. \quad (2.89)$$

Now we can use equation (2.2) to solve for the induced effective pressure of the system due to the dependence on t of the effective mass. Once again expanding $p_{eff} = p_{0,eff} + r^2 p_{2,eff} + \dots$ we find

$$p_{0,eff} = -\frac{9M_0^2}{a_0^6 \rho_{cr}}, \quad (2.90)$$

$$p_{2,eff} = -\frac{18M_0 M_2}{a_0^6 \rho_{cr}} + \frac{54M_0^2 a_2}{a_0^7 \rho_{cr}}. \quad (2.91)$$

Equations (2.4) and (2.5) give

$$\nu' = -\frac{p'_{eff}}{\rho_{eff} + p_{eff}} = -\frac{2p_{2,eff}}{\rho_{eff} + p_{eff}} r + \dots, \quad (2.92)$$

$$\Rightarrow \nu = \nu_2 r^2 + \dots = -\frac{p_{2,eff}}{\rho_{0,eff} + p_{0,eff}} r^2 + \dots, \quad (2.93)$$

$$= \frac{6M_0}{a_0^3 \rho_{cr}} \left(\frac{\frac{M_2}{M_0} - \frac{3a_2}{a_0}}{1 - \frac{6M_0}{a_0^3 \rho_{cr}}} \right) r^2. \quad (2.94)$$

For $r \rightarrow 0$, in the marginally bound case,

$$G = b(r) e^{2rA}, \quad (2.95)$$

$$\simeq 1 + 2A_2 r^2, \quad (2.96)$$

where A is defined by (from equation (2.5))

$$\dot{A} := \nu' \frac{\dot{R}}{R'} = 2\nu_2 \frac{\dot{a}}{a + r a'} r^2 = \dot{A}_2 r^2 + \dots, \quad (2.97)$$

$$\Rightarrow A_2 = 2 \int_0^t \nu_2 \frac{\dot{a}_0}{a_0} d\bar{t}. \quad (2.98)$$

This model provides everything required to solve the equation of motion for the scale parameter a which comes from equation (2.6). It can be rewritten as

$$M_{eff} = a \left(\frac{1-G}{r^2} + e^{-2\nu \dot{a}^2} \right), \quad (2.99)$$

$$= (a_0 + a_2 r^2) (-2A_2 + e^{-2\nu_2 r^2} (\dot{a}_0 + \dot{a}_2 r^2)^2), \quad (2.100)$$

$$\Rightarrow M_{0,eff} = a_0 (-2A_2 + \dot{a}_0^2), \quad (2.101)$$

$$\Rightarrow M_{2,eff} = a_2 (-2A_2 + \dot{a}_0^2) + 2a_0 (\dot{a}_0 \dot{a}_2 - \nu_2 \dot{a}_0^2). \quad (2.102)$$

In the limit of $\rho_{cr} \rightarrow \infty$, we retrieve the classical inhomogeneous collapse model with $\nu_2 \rightarrow 0, M_{0,eff} \rightarrow M_0, M_{2,eff} \rightarrow M_2$, and in the limit of $M_2 \rightarrow 0$ we return to the quantum homogeneous model discussed previously. We now have a model which satisfies the 2 conditions originally laid out.

Combining these equation with (2.88) and (2.89), we get the equations of motion for the scale factor that need to be solved.

$$\dot{a}_0^2 = \frac{M_0}{a_0} \left(1 - \frac{3M_0}{a_0^3 \rho_{cr}} \right) + 2A_2, \quad (2.103)$$

$$\dot{a}_2^2 = \frac{M_2}{2a_0 \dot{a}_0} \left(1 - \frac{6M_0}{a_0^3 \rho_{cr}} \right) - \frac{M_0 a_2}{2a_0^2 \dot{a}_0} \left(1 - \frac{12M_0}{a_0^3 \rho_{cr}} \right) + \nu_2 \dot{a}_0. \quad (2.104)$$

This analysis is valid in the small r limit, where we assume higher order terms are negligible, but this breaks down at a certain radius for any given M_2 and ρ_{cr} . The other issue is that of shell crossing singularities, where $R' = 0$ and different collapsing shells overlap, but as discussed before these are weak singularities and do not signal geodesic incompleteness of the spacetime. This situation is complicated by the fact that outgoing shells which have already reached the bounce point could overlap with in-falling shells, causing more shell-crossing singularities, however in the model discussed here the bounce occurs first at the outer-most shells, so if shells crossings do occur they are outside the small r limit.

2.3.5 Apparent Horizon

In this model the collapsing cloud is affected one shell at a time due to the inhomogeneities, and the bounce time will be different for each shell. The bounce curve $t_{cr}(r)$ is defined from $\dot{a}(r, t_{cr}(r)) = 0$, and in contrast to the homogeneous case, $t_{cr}(r)$ is not a constant. This will mean the region of asymptotic freedom is reached at different times for each shell, and so the gravity never completely turns off. Importantly, the outer shells bounce before the inner shells, meaning there are no shell crossing singularities near the center. The fact t_{cr} is not constant also means the effective density doesn't reach 0, as opposed to the homogeneous case where $\rho_{eff}(t_{cr}) = 0$. The effective density still decreases as we approach the bounce.

This process looks similar to the case for the homogeneous dust collapse model earlier, but the apparent horizon never full disappears.

The apparent horizon condition is still given by $F = R$, so the time $t_{ah}(r)$ at which shell r becomes trapped is given implicitly by

$$a(r, t_{ah}(r)) = r^2 M_{eff}(r, t_{ah}(r)), \quad (2.105)$$

$$\Rightarrow a_0 + a_2 r^2 = r^2 (M_{0,eff} + M_{2,eff} r^2), \quad (2.106)$$

while we can invert this to find t_{ah} explicitly through

$$r^4 M_{2,eff} + r^2 (M_{0,eff} - a_2) - a_0 = 0 \quad (2.107)$$

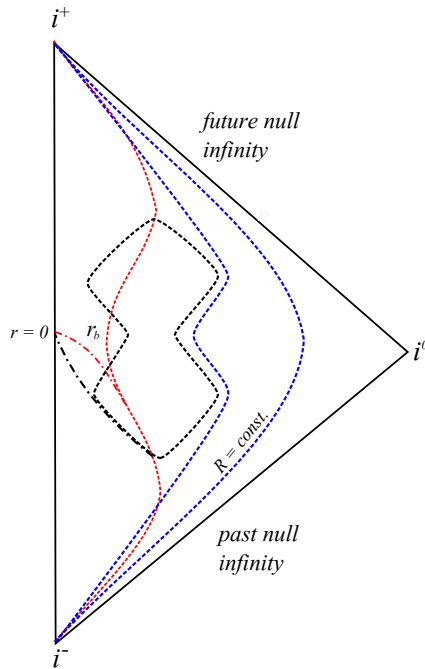


Figure 2.4: **Quantum Corrected Inhomogeneous Dust Collapse**

Penrose diagram for the semiclassical inhomogeneous dust collapse model discussed above.

The black lines correspond to the trapped surface of the collapsing object. The red dotted line is the boundary curve of the collapsing object. The dashed-dotted black and red lines correspond to the classical collapse case. At some point after the collapse starts the quantum effects kick in, and the semiclassical solution departs from the classical singularity formation, however in contrast with the homogeneous model, the bounce point is never visible to an observer at infinity as the apparent horizon does not vanish until the very end.

Like the homogeneous case the apparent horizon will behave classically in the weak field regime and reaches a minimum r_{min} at time t_{min} given by $\dot{r}_{ah}(t_{min}) = 0$.

Once again we have shown that, as opposed to the classical picture in which collapse inevitably leads to singularity formation, this final outcome can be avoided by including the semi-classical corrections discussed above. The singularity never forms, and instead the end stage is a process of re-expansion of the cloud, solving related problems such as non-unitarity. The fact that no event horizon forms arises from the fact that the exterior spacetime of the star is not described by a Schwarzschild metric, but instead a Vaidya spacetime where the solutions are matched at the boundary.

3 Perfect Fluid Models of Gravitational Collapse

3.1 Homogeneous Perfect Fluid Collapse

In this section, we will analytically study spherical gravitational collapse models of a perfect fluid, under an equation of state condition $p = k\rho$. This equation of state is extensively used and studied in astrophysics, and offers a physically interesting model. This equation of state will apply an additional constraint to the collapsing matter, on top of the Einstein equations. We will see how applying a physically reasonable equation of state affects the collapse evolution, and how the final stage of the process is affected by it as the pressures cannot be ignored in the later stages of collapse.

We will show that the perfect fluid collapse model could end in either a black hole or naked singularity, depending on the nature of the initial data and how it evolves during the collapse process. Given regular initial data the final stage will be determined by the choice of free functions in the theory, such as initial velocity of the collapsing matter and we will see how the equation of state and initial data affect the outcome of the collapse process. Much of the preliminary work has been done in the previous section, so I will give only a brief recap here, but I will elaborate further on any new or unique points.

We start with the spherically symmetric metric in comoving coords (t, r, θ, ϕ)

$$ds^2 = -e^{2\nu} dt^2 + e^{2\psi} dr^2 + R^2 d\Omega^2. \quad (3.1)$$

The energy-momentum tensor for a perfect fluid in this frame is given by

$$T^{ij} = (\rho + p)V^i V^j + pg^{ij}, \quad (3.2)$$

where V^i is a timelike vector.

$$\Rightarrow T_t^t = -\rho(r, t) \text{ and } T_r^r = T_\theta^\theta = T_\phi^\phi = p(r, t). \quad (3.3)$$

Taking the matter to satisfy the weak energy condition, we have that

$$\begin{aligned} T_{ij}V^i V^j &\geq 0, \\ \Rightarrow \rho &\geq 0 \text{ and } \rho + p \geq 0. \end{aligned}$$

From equations (2.2) and (2.3), and using the equation of state, we have

$$\rho(r, t) = \frac{F'}{R^2 R'} = -\frac{1}{k} \frac{\dot{F}}{R^2 \dot{R}} = -\frac{1}{k} p(r, t), \quad (3.4)$$

and from our other initial equations

$$\nu' = -\frac{k}{k+1} \frac{\rho'}{\rho} = -\frac{k}{k+1} [\ln(\rho)]' \quad (3.5)$$

$$\dot{G} = 2 \frac{\nu'}{R'} \dot{R} G \quad (3.6)$$

$$F = R(1 - G + H) \quad (3.7)$$

From the energy conditions, the MS mass function $F \geq 0$, and to preserve initial regularity, we have $F(t_i, 0) = 0$, meaning the mass function vanishes at the center. Again, for collapse $\dot{R} < 0$ where $R(r, t) = ra(r, t)$, and $a(r, t_i) = 0, a(r, t_s(r)) = 1$. This allows us to distinguish the point at which the physical radius vanishes, and the singularity at time $t_s(r)$. We now have five field equations, and five unknowns in ρ, ψ, ν, R , and F . These equations, subject to the energy and regularity conditions discussed, determine the evolutions of the initial data into the final states of collapse.

We will see there are different classes of solutions which end in either a black hole or naked singularity as the final stage of collapse, depending on the initial data configurations and class of evolution chosen.

3.1.1 Collapsing Matter Clouds

We will now examine the equations to see when the spacetime singularity occurs, and how the initial data and evolution classes lead to a singularity being formed in the spacetime. Given

$$F(r, t) = r^3 M(r, a),$$

where M is suitably regular and differentiable, and since M is a general (at least \mathcal{C}^2) function, we have a very generic form of the mass profile for the cloud. Equation (3.4) gives

$$\rho(r, a) = \frac{3M + r(M_{,r} + M_{,a}a')}{a^2(a + ra')} = -\frac{1}{k} \frac{M_{,a}}{a^2} = -\frac{1}{k} p(r, a). \quad (3.8)$$

A regular distribution at the initial epoch is given by

$$\rho(r, 0) = 3M(r, 1) + rM(r, 1)_{,a}. \quad (3.9)$$

It is clear from these equations that, generally, as $a \rightarrow 0, \rho \rightarrow \infty$, and both the pressure and density blow up at the singularity. Rewriting equation (3.8) gives

$$3kM + krM_{,r} + Q(r, a)M_{,a} = 0, \quad (3.10)$$

where

$$Q(r, a) = (k + 1)ra' + a.$$

Equation (3.10) above has a general solution of the form [28]

$$\mathcal{F}(X, Y) = 0,$$

where $X(r, a, M)$ and $Y(r, a, M)$ are the solutions of the system of equations

$$\frac{dM}{3Mk} = \frac{dr}{kr} = \frac{da}{Q}.$$

From all the classes of solutions of $M(r, a)$, we only consider those which satisfy the constraints outlined earlier, i.e. the energy condition, regularity, and in the limit $a \rightarrow 0, \rho \rightarrow \infty$. This limits the class of mass functions we need to examine.

Integrating (3.5)

$$\Rightarrow \nu = -\frac{k}{k+1} \ln(\rho). \quad (3.11)$$

Using $A(r, a)_{,a} := \nu'/R'$ as before, we can determine the regularity of our solutions. Our main interest is again analyzing the shell-focusing singularity at $R = 0$, which is a physical singularity. Again we are assuming there are no shell-crossing singularities, where $R' = 0$, ensuring the function $A(r, a)$ is well defined.

Initially we have

$$A(r, a)_{,a}|_{a=1} = -\frac{k}{k+1} \left[\frac{\rho'_0(r)}{\rho_0(r)} \right] \quad (3.12)$$

and at any stage of the collapse we can relate the functions M and A by

$$A_{,a}R' = -\frac{k}{k+1} \ln\left[-\frac{M_{,a}}{ka^2}\right]'$$

Considering a smooth initial profile, where initial density gradient is zero at the center, we must have $A(r, a) = rg(r, a)$, where $g(r, a)$ is also suitably differentiable [28].

We also have

$$G(r, a) = b(r)e^{2rA}, \quad (3.13)$$

where

$$b(r) = 1 + r^2 b_0(r), \quad (3.14)$$

and $b(r)$ is the velocity function for collapsing shells. As shown in equation (2.20), we can use equation (2.6) to get

$$\begin{aligned} b(r)e^{2rA} - e^{-2\nu} \dot{R}^2 &= 1 - \frac{F}{ra} \\ \Rightarrow \sqrt{a}\dot{a} &= -\rho^{-\frac{k}{k+1}} \sqrt{e^{2rA} ab_0(r) + ah(r, a) + M(r, a)}, \end{aligned} \quad (3.15)$$

with $h(r, a) = \frac{e^{2rA}-1}{r^2}$, giving

$$\Rightarrow t(r, a) = \int_a^1 \frac{\sqrt{\tilde{a}} d\tilde{a}}{\rho^{-\frac{k}{k+1}} \sqrt{b_0(r) a e^{2rA} + ah(r, \tilde{a}) + M(r, \tilde{a})}}. \quad (3.16)$$

Close to the center

$$t(r, a) = t(0, a) + r\chi(a) + O(r^2). \quad (3.17)$$

When $t(r, a)$ is differentiable, we Taylor expand near $r = 0$, and the above integral is evaluated at $r = 0$ where

$$\chi(a) = \frac{dt}{dr} = -\frac{1}{2} \int_a^1 d\tilde{a} \frac{\sqrt{\tilde{a}} B_1(0, \tilde{a})}{B(0, \tilde{a})^{\frac{3}{2}}}, \quad (3.18)$$

with

$$\sqrt{B(r, a)} = \rho^{-\frac{k}{k+1}} \sqrt{b_0(r) a e^{2rA} + ah(r, \tilde{a}) + M(r, \tilde{a})}, \quad (3.19)$$

$$B_1(r, a) = B_{,r}(r, a). \quad (3.20)$$

To obtain (119) we required that the integral (118) be differentiable, which is possible because it is finite by definition, and as long as all the functions $A(r, a)$, $b_0(r)$, and $M(r, a)$ are suitably differentiable. They must be at least \mathcal{C}^2 for $r \neq 0$, and \mathcal{C}^1 for $r = 0$. The central shell will reach the singularity in a time

$$t_{s_0} = \int_0^1 \frac{\sqrt{a} da}{B(0, a)}. \quad (3.21)$$

For other shells to reach the singularity it will take a time

$$t_s(r) = t_{s_0} + r\chi(0) + O(r^2), \quad (3.22)$$

which defines the singularity curve that develops in the spacetime as a result of the collapse. From equation (3.15) - (3.18)

$$\sqrt{a}\dot{a} = \chi(a)B(0, a) + O(r^2). \quad (3.23)$$

We can see that $\chi(0)$, representing the singularity curve tangent, depends on M , b_0 , and h , which are determined by values of the initial data at $t = t_i$. Given the density and matter profiles initially is therefore enough to completely determine the tangent to the singularity curve at the center. We now have to figure out the nature of the singularity, and determine when it will be naked and when it will become a black hole.

3.1.2 Nature of the Singularity

We can now determine the final stage of collapse as either a naked singularity or a black hole, using the initial data and allowed evolutions. Once again, the apparent horizon is given by $R = F$ within the collapsing cloud, and if the area around the center gets trapped before the singularity, it will be covered and a black hole will form, otherwise future-directed null/timelike curves can escape and we will have a locally or globally naked singularity. We now examine whether there exist families of future directed and outgoing null geodesics which terminate in the past at the singularity.

We first consider the equation for the null radially outgoing geodesics, given by

$$\frac{dt}{dr} = e^{\psi-\nu}, \quad (3.24)$$

where the singularity is given by $a(t_s(r), r) = 0 \Rightarrow R(t_s(r), r) = 0$. If any future directed null geodesics exist which originate from the singularity in the past, we must have $R \rightarrow 0$ as $t \rightarrow t_s$. Writing the geodesic equation in terms of $(u = r^\alpha, R)$ [28], we get

$$\frac{dR}{du} = \frac{1}{\alpha} r^{-(\alpha-1)} R' \left[1 + \frac{\dot{R}}{R'} e^{\psi-\nu} \right]. \quad (3.25)$$

From equation (2.6) we find that

$$1 + \frac{\dot{R}}{R'} e^{\psi-\nu} = \frac{1 - \frac{F}{R}}{\sqrt{G}(\sqrt{G} - \sqrt{H})}, \quad (3.26)$$

and taking $\alpha = \frac{5}{3}$ [16] we get

$$\frac{dR}{du} = \frac{3}{5} \left(\frac{R}{u} + \frac{\sqrt{aa'}}{\sqrt{\frac{R}{u}}} \right) \left(\frac{1 - \frac{F}{R}}{\sqrt{G}(\sqrt{G} - \sqrt{H})} \right). \quad (3.27)$$

If null geodesics exist that terminate at the singularity in the past and have a definite tangent, then $\frac{dR}{du} > 0$ at the singularity in the (u, R) plane and has a finite value. So all points $r > 0$ are covered, because the apparent horizon equation $F/R \rightarrow \infty$ as $dR/du \rightarrow -\infty$, and $\sqrt{H} < 0$ since $\dot{R} < 0$ for collapse. This means that no null outgoing geodesics can originate from these past points.

However, the $r = 0$ singularity could be naked. Defining the tangent to null outgoing geodesics as

$$x_0 = \lim_{t \rightarrow t_s} \lim_{r \rightarrow 0} \frac{R}{u} = \left. \frac{dR}{du} \right|_{t \rightarrow t_s; r \rightarrow 0}. \quad (3.28)$$

Using (3.27) and (3.23) we have

$$x_0 = \frac{3}{5} \left(x_0 + \frac{\chi(0)\sqrt{B(0,0)}}{x_0^{1/2}} \right), \quad (3.29)$$

$$\Rightarrow x_0^{3/2} = \frac{3}{2} \chi(0) \sqrt{B(0,0)}. \quad (3.30)$$

We now examine the necessary/sufficient condions for the existence of a naked singularity. The equation for the null geodesic emerging from the singularity is $R = x_0 u$, which in (t, r) coordinates, this is equivalent to

$$t_s(r) = t_s(0) + x_0 r^{5/3}.$$

If $\chi(0) > 0 \Rightarrow x_0 > 0$, and we have a null radially outgoing geodesic escaping from the singularity, resulting in a naked singularity, however if $\chi(0) < 0$, then obviously the singularity curve is a decreasing function of r , and therefore the central region will become singular before the central shell resulting in a black hole solution. This is because the central region is always covered by an apparent horizon. If $\chi(0) = 0$ we must account for the next highest order non-zero term in the singularity curve equation, with a similar analysis for a different value of α .

We know that the behaviour of $\chi(0)$ is entirely determined by the initial conditions, as shown in equation (3.18), so it is possible to determine the end state as either a black hole or

naked singularity purely from the initial data and dynamical evolution of the system. Given any regular density and pressure profiles, we can always choose velocity profiles so that the end state is one or the other.

The general result here shows that for any perfect fluid case with $p = k\rho$ as the equation of state, the value of k doesn't have any special significance. The initial data and the chosen evolutions are the things that matter, which will result in a certain final stage.

3.1.3 Classic Radiation Model

This classic FRW solution describes the collapse of a homogeneous perfect fluid, with $p_r = p_\theta = p(t)$, where we have an equation of state governing radiation as

$$\rho = 3p. \quad (3.31)$$

The homogeneous pressure in this case means the mass profile must depend on t throughout the collapse, and can be matched with Vaidya solution on the exterior [30], [31]. This equation of state, along with equation (3.4), will give us a differential equation for the mass profile

$$\frac{dM}{da} = -\frac{M}{a}, \quad (3.32)$$

$$\Rightarrow M(t) = \frac{M_0}{a}. \quad (3.33)$$

We then have an energy density $\rho = \frac{3M_0}{a^4}$, and in the marginally bound case the equation of motion (3.7) becomes

$$M_0 = a^2 \dot{a}^2, \quad (3.34)$$

$$\Rightarrow a(t) = (1 - 2\sqrt{M_0}t)^{1/2}. \quad (3.35)$$

At $a(t) = 0 \Rightarrow t_s = 1/2\sqrt{M_0}$, and the end stage of the process results in a black hole.

3.2 Inhomogeneous Perfect Fluid Collapse

We will now try to make a more physically realistic collapse scenario by including inhomogeneities in the density and pressure profiles of the collapsing fluid model. After this, we can examine the possible outcomes of the collapse, and show how unstable the currently theorized process is because it is just as likely to end in a naked singularity as it is to end in a black hole. If the Cosmic Censorship Conjecture is to hold, this points to something fundamentally flawed in our current ideas, since the process must be very fine tuned to definitely result in a black hole.

To do this, the currently known models are considered under small perturbations of the initial data, and we want to see how stable the black hole solutions are under these perturbations. In the dust case already examined, we have already seen how drastically the outcomes of collapse can be affected by these perturbations, and that we must consider naked singularities just as stable and general an outcome as black holes.

Following [37] we begin with regular initial data that has no trapping horizons or singularity, and then introduce small inhomogeneities into the pressure profile of a perfect fluid. We will not use an equation of state, but still require that it obeys the energy conditions.

3.2.1 Introducing Inhomogeneities

From the Einstein equations (2.2)-(2.6), we have our usual five equations with six unknowns. We will not specify an equation of state here, leaving the mass profile M as the free function, and consider matter that acts classically in the weak field limit. To examine the inhomogeneities in the density and pressure radial inhomogeneities are introduced in the mass, giving $M(t) \rightarrow M(t, r)$. This is a physically reasonable assumption for any collapsing object, as it should be most dense in the center, and decrease radially outward. This also causes $a(t) \rightarrow a(t, r)$, allowing us to change coords from $(r, t) \rightarrow (r, a)$ as earlier. Since a is a function of r and t , any radial derivatives will become $X' = X_{,r} + X_{,a}a'$.

The pressure and density inhomogeneities are introduced in [37] as

$$p(a, r) = p_0(a) + p_1(a)r + \frac{1}{2}p_2(a)r^2, \quad (3.36)$$

$$\rho(a, r) = \rho_0(a) + \rho_1(a)r + \frac{1}{2}\rho_2(a)r^2, \quad (3.37)$$

where $p_i(a), \rho_i(a)$ depend on the specific form of M . They then choose the Misner-Sharp mass F so the M is separable in r and a as

$$M(r, a) = m(a)(1 + \epsilon(r)), \quad (3.38)$$

where ϵ is the radial perturbation of $M(r, a)$, and is "small" compared to $m(a)$. For regularity and continuity, we assume M is at least \mathcal{C}^2 in r and \mathcal{C}^1 in a , and again see that

$$M(r, a) = M_0(a) + M_1(a)r + \frac{1}{2}M_2(a)r^2. \quad (3.39)$$

Similar to the dust case, to prevent cusps at the origin and ensure regularity of data, M_1 must vanish at $r = 0$. Thus, $M_1(a) = m(a)\epsilon'(0) = 0 \Rightarrow \epsilon'(0) = 0$. Fixing another gauge allows us to assume $\epsilon(0) = 0$, ensuring the center of the cloud acts in the same way as the homogeneous fluid collapse model. The final requirement is for $|M_2| \ll M_0$, giving $\epsilon''(0) \ll 1$.

The continuity of M means we can take $m(a)$ to be of the form [37]

$$m(a) = m_0 + m_1 a. \quad (3.40)$$

Expanding the pressure and density about $r = 0$ in equations (2.2) and (2.3) gives

$$p(a, r) = -\frac{m(a),a}{a^2} - \frac{1}{2} \frac{m(a),a}{a^2} \epsilon''(0) r^2, \quad (3.41)$$

$$\rho(a, r) = \frac{3m(a)}{a^3} + \frac{5}{2} \frac{m(a)\epsilon''(0)}{a^2} r^2. \quad (3.42)$$

For a realistic model in which density decreases radially outward, we must have $\epsilon''(0) < 0$.

Using the mass equation of motion (2.6), we can simplify it to find the equation of motion of the system, as previously shown, to be

$$\dot{a} = -e^\nu \sqrt{\frac{M}{a} + \frac{be^{2A} - 1}{r^2}}, \quad (3.43)$$

which will completely solve the system for given choices of M and b . In the marginally bound case we have been discussing, $b(r) = 1$.

From equation (2.4)

$$\nu(r, a) = \int_0^r -\frac{p'}{\rho + p} dr, \quad (3.44)$$

$$= \int_0^r \frac{M_{,ra}a + (M_{,aa}a - 2M_{,a})a'}{(3M + rM_{,r} - aM_{,a})a} R' d\tilde{r}, \quad (3.45)$$

and defining $A_{,a} := \nu' r / R'$, we have that

$$A(r, a) = \int_a^1 \frac{M_{,ra}a + (M_{,aa}a - 2M_{,a})a'}{(3M + rM_{,r} - aM_{,a})a} r da. \quad (3.46)$$

Given the expansion around $r = 0$ for M , we find a corresponding expansion for $A(r, a)$ as $A = A_0(a) + A_1(a)r + A_2(a)r^2 + A_3(a)r^3 + A_4(a)r^4 + \dots$, and checking the r^2 coefficient from the above integral for A using the expansion of the mass profile, we find [37]

$$A_2(a) = \int_a^1 \frac{2M_{2,a}}{(3M_0 - M_{0,a})} da = \frac{2}{3} \frac{m_1 \epsilon''(0)}{m_0} (1 - a). \quad (3.47)$$

Inverting (3.43) as usual, the time curve is defined as

$$t(r, a) = t_i + \int_a^1 \frac{e^{-\nu} \sqrt{a}}{\sqrt{M + 2A_2 a + 2r^2 A_4 a}} da. \quad (3.48)$$

Again, regularity of the functions in $t(r, a)$ means it is generally at least \mathcal{C}^2 near $r = 0$ and can also be expanded as

$$t(r, a) = t(0, a) + \chi_1(a)r + \chi_2(a)r^2 + O(r^3), \quad (3.49)$$

with $\chi_1 = dt/dr|_{r=0}$ and $\chi_2 = \frac{1}{2}d^2t/dr^2|_{r=0}$. The singularity curve $t_s(r)$, defined as $t_s(r) = t(r, 0)$, which is the time taken for a shell of radius r to collapse to the singularity, can also be expanded as

$$t_s(r) = t(0, 0) + \chi_1(0)r + \chi_2(0)r^2 + O(r^3). \quad (3.50)$$

3.2.2 Nature of the Singularity

As shown in Section (2.2.3) and [22], since $M_1 = 0 \Rightarrow \chi_1(0) = 0$, and it is the value of $\chi_2(0)$ which governs the nature of the singularity. If $\chi_2(0) > 0$, $t_s(r)$ is always increasing in co-moving time t , so the singularity is first formed at the central $r = 0$ shell. As in Section (2.1.4), for a black hole to form we require that the trapping horizon forms before the singularity, $t_{ah}(r) \leq t_s(0)$. So the positivity of $\chi_2(0) \Rightarrow t_{ah}(r) > t_s(0)$, which means null geodesics could escape from the singularity forming at $t_s(0)$. At least locally, this results in a naked singularity.

Solving for $\chi_2(0)$, only keeping terms to the order of $\frac{m_1}{m_0}$, this becomes [37]

$$\chi_2(0) = - \int_0^1 \frac{\epsilon''(0)}{m_0^{1/2}} \left[\frac{a^{1/2}}{2} + \frac{m_1}{m_0} \left(\frac{7}{12} a^{3/2} - \frac{\epsilon''(0)}{m_0} (a^{3/2} - a^{5/2}) \right) \right] da. \quad (3.51)$$

After solving the integral, and ignoring the last term due to to smallness of powers of a near $r = 0$, we find

$$\chi_2(0) = - \frac{\epsilon''(0)}{3m_0^{1/2}} \left(1 + \frac{7}{10} \frac{m_1}{m_0} \right). \quad (3.52)$$

As already mentioned, a physically reasonable profile requires $\epsilon''(0) < 0$, so the sign of $\chi_2(0)$ is determined entirely by the value of the quantity in brackets. For small perturbations of an otherwise homogeneous fluid model, we can safely assume that $m_0 < m_1 \Rightarrow \left| \frac{m_1}{m_0} \right| < 1$. Therefore, regardless of the sign of m_1 , the bracketed term is always positive, which implies that the value of $\chi_2(0) > 0$ for any initial data, so it is safe to conclude that for any scenario in which we make small perturbations from the homogeneous perfect fluid collapse model the end state of collapse must result in a locally naked singularity.

In a very similar way to the inhomogeneous dust collapse model, we have shown that by introducing small pressure perturbations to the collapse model we can change the outcome quite remarkably. I think it is safe to assume that in the extremely dynamic process of a star undergoing gravitational collapse, the pressures and forces would fluctuate wildly. Once again we are left with an end state of collapse in the form of a naked singularity, and once again we have to resolve this problem if the process is to obey the Cosmic Censorship Conjecture.

3.3 Non-Singular Fluid Collapse

3.3.1 Radiating Star Model

Beginning with the usual five equations and six unknowns, ρ, p, ψ, ν, R , and F , this allows us the liberty to choose a free function. The selection of this function, subject to certain initial data and energy conditions, determines the evolution of the spacetime. We will choose this to be $F(r, t)$, the mass function for the cloud. The cloud has a compact support on a $t = \text{const}$ spacelike hypersurface, and the exterior spacetime is matched to the boundary of the collapsing ball.

We consider the class of mass functions $F(r, t)$, in which $M(r, a)$ is a general function subject to some physicality conditions [29]:

1. $M(r, a) \geq 0$ and $M(r, a)$ is at least \mathcal{C}^2 .
2. $\lim_{a \rightarrow 0} M \rightarrow 0$ as a^α , with $1 < \alpha < 3$.
3. There exists a value $a^* \in (0, 1)$, such that $M_{,a}|_{a>a^*} < 0$, $M_{,a}|_{a<a^*} > 0$, and $M_{,a}|_{a=a^*} = 0$.

Subject to these conditions, it is clear from $p = -\frac{M_{,a}}{a^2}$ that at the initial stage of collapse the pressure is positive, but as it continues the pressure will decrease and eventually become negative in a region around the singularity. For this model we will impose the continual collapse condition $\dot{R} < 0$, and in the next section discuss the case where the collapsing system bounces back and re-expands.

The pressure is positive for all $a > a^*$, becoming negative where $a < a^*$. When $a = a^*$ it acts like a pressureless dust. The apparent horizon is the boundary of the trapped area, and determines whether or not a black hole forms during the collapse, given by $F = R$. When $F < R$, the region described is not trapped, while $F > R$ is where the region is trapped. Regularity of the initial data would suggest there are no trapped surfaces to begin with, and if $r = r_b$ is the boundary of the cloud, the condition $(M_0)r_b^2 < 1$ will ensure there are no trapped surfaces for $r \leq r_b$ because $F/R < 1$ is preserved.

Basically, we can view the formation of trapped surfaces by how much mass is within a given radius of the cloud. This determines whether there is a trapped surface or not. If $F > R$ tells us a trapped surface will form, the star must have some mechanism for radiating away mass as R decreases, to preserve $F < R$ throughout.

Given the general conditions discussed for this model, as $a \rightarrow 0$

$$\frac{F}{R} \simeq r^2 a^{\alpha-1} = 0, \quad (3.53)$$

therefore, even as the collapse ends and the physical radius $r \rightarrow 0$ there are no trapped surfaces forming in our spacetime. This is because because the induced negative pressure means at some point \dot{F} becomes less than zero. This implies the mass function decreases in time, and as the process continues the mass is radiated away, there is never enough mass within a given radius to allow trapped surfaces to form. When we reach $a = 0 \Rightarrow F = 0$, and all the mass has been radiated away. We have a class of gravitational collapse models with

regular initial data, a reasonable form of matter, and that satisfy the energy conditions, such that trapping is avoided.

We can now match this set of non-singular perfect fluid solutions with an exterior Vaidya metric. A Vaidya metric is a generalization of Eddington-Finkelstein coordinates to a case in which the mass is not constant, but is a function of the coordinate time, $M = M(v)$. We can then match this metric to the interior metric discussed above at the boundary hypersurface Σ given by $r = r_b$. This hypersurface divides the spacetime into two separate four-dimensional manifolds \mathcal{V}^+ and \mathcal{V}^- . The metric of \mathcal{V}^- inside of Σ is given by

$$ds_-^2 = -e^{2\nu} dt^2 + e^{2\psi} dr^2 + R^2 d\Omega^2, \quad (3.54)$$

and outside of Σ we have \mathcal{V}^+ , the generalised Vaidya metric

$$ds_+^2 = - \left(1 - \frac{2M(r_v, v)}{r_v} \right) dv^2 - 2dvdr_v + r_v^2 d\Omega^2, \quad (3.55)$$

where v is the retarded null coordinate and r_v is the Vaidya radius. At the boundary the Vaidya radius equals the area radius

$$R(r_b, t) = r_v(v), \quad (3.56)$$

so that on Σ we have

$$ds_{\Sigma-}^2 = -e^{2\nu} dt^2 + R^2 d\Omega^2, \quad (3.57)$$

$$ds_{\Sigma+}^2 = - \left(1 - \frac{2M(r_v, v)}{r_v} + 2 \frac{dr_v}{dv} \right) dv^2 + r_v^2 d\Omega^2. \quad (3.58)$$

When approaching Σ in \mathcal{V}^+ or \mathcal{V}^- , we must have [30]

$$ds_{\Sigma-}^2 = ds_{\Sigma+}^2 = ds_{\Sigma}^2. \quad (3.59)$$

Matching the first fundamental forms gives

$$\left(\frac{dv}{dt} \right)_{\Sigma} = \frac{e^{\nu}}{\sqrt{1 - \frac{2M(r_v, v)}{r_v} + 2 \frac{dr_v}{dv}}}, \quad (3.60)$$

$$(r_v)_{\Sigma} = R(r_b, t). \quad (3.61)$$

The second continuity equation imposed on Σ comes from matching the second fundamental forms [29]

$$[K_{ab}] = K_{ab}^+ - K_{ab}^- = 0, \quad (3.62)$$

where K_{ab} is the external curvature of the metric. We can calculate the normal to the hypersurface Σ in each metric system, using $n^\mu = g^{\mu\nu} \partial_\nu \Sigma$ at the boundary of the surface. In the interior we have

$$n_-^i = (0, e^{-\psi}, 0, 0), \quad (3.63)$$

and in the exterior Vaidya spacetime we have components

$$n_+^v = -\frac{1}{\sqrt{1 - \frac{2M(r_v, v)}{r_v} + 2\frac{dr_v}{dv}}}, \quad (3.64)$$

$$n_+^{r_v} = \frac{1 - \frac{2M(r_v, v)}{r_v} + \frac{dr_v}{dv}}{\sqrt{1 - \frac{2M(r_v, v)}{r_v} + 2\frac{dr_v}{dv}}}. \quad (3.65)$$

Defining the extrinsic curvature as

$$K_{ab} = \frac{1}{2}\mathcal{L}_{\mathbf{n}}g_{ab} = \frac{1}{2}[g_{ab,c}n^c + g_{cb}n_{,a}^c + g_{ac}n_{,b}^c]. \quad (3.66)$$

From the second continuity equation above, we set $K_{\theta\theta}^-|_{\Sigma} = K_{\theta\theta}^+|_{\Sigma}$ which gives us

$$RR'e^{-\psi} = r_v \frac{1 - \frac{2M(r_v, v)}{r_v} + \frac{dr_v}{dv}}{\sqrt{1 - \frac{2M(r_v, v)}{r_v} + 2\frac{dr_v}{dv}}}. \quad (3.67)$$

From equation (3.60), (3.61), and then defining $F(r_b, t) = 2M(r_v, v)$ we can simplify this to

$$RR'e^{-\psi} = R\left(1 - \frac{F(r_b, t)}{R(r_b, t)} + \frac{dR}{dv}\right)e^{-\nu}\frac{dv}{dt}\Big|_{\Sigma}, \quad (3.68)$$

$$\Rightarrow \frac{dv}{dt}\Big|_{\Sigma} = \frac{e^{\nu}(R'e^{-\psi} - \dot{R}e^{-\nu})}{1 - \frac{F}{R}}. \quad (3.69)$$

Setting $K_{\tau\tau}^- = K_{\tau\tau}^+$, with τ the proper time on Σ , we finally get

$$M(r_v, v)_{,r_v} = \frac{F}{2R} + \frac{Re^{-\nu}}{\sqrt{G}}\sqrt{G}_{,t} + Re^{2\nu}\nu'e^{-\psi}, \quad (3.70)$$

where $G = e^{-2\psi}(R')^2$ and $H = e^{-2\nu}\dot{R}^2$ as before.

Any mass function $M(r_v, v)$ from the Vaidya metric which satisfies this equation will have a unique exterior spacetime with required equations of motion given by the matching conditions (3.56) and (3.69) [29]. Some examples of this type of mass function would be a charged Vaidya spacetime as the exterior, where $M = M(v) + Q(v)/r_v$, or an anisotropic de Sitter exterior where $M = M(r_v)$, which are both solutions of (3.70) [17].

Since the condition $F(r_b, t) = 2M(r_v, v)$ gives the value of M at the boundary, and (3.70) gives the value of the partial derivative with respect to r_v at the boundary, the value of the partial derivative with respect to v is still free, so our equations in fact give a class of generalized exterior Vaidya mass functions.

Along the singularity curve $t \rightarrow t_s$, we have that

$$\lim_{r_v \rightarrow 0} \frac{2M(r_v, v)}{r_v} \rightarrow 0,$$

therefore the exterior metric along the singularity curve will transform to

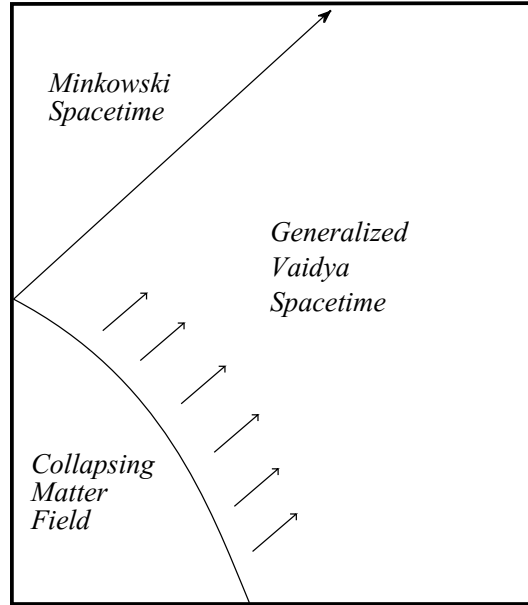


Figure 3.1: **A Schematic Diagram of the Radiating Star Process**

$$ds^2 = -dv^2 - 2dvdr_v + r_v^2 d\Omega^2.$$

This is the Minkowski metric in retarded null coordinates, i.e. flat spacetime.

We have shown here that as opposed to the naked singularity solutions or black hole solutions discussed earlier, the Einstein equations readily admit solutions where a singularity is not the final state of gravitational collapse, solving a lot of the paradoxical problems that are associated with black holes such as information loss and violations of the unitarity principle.

3.3.2 Quantum-Corrected Homogeneous Radiation Model

In this section we will use an alternative non-singular collapse process, where we try to rewrite Einstein's equation as a radiation + corrections mode, and ρ_{cr} once again indicates where the corrections become relevant. Taking [24]

$$\rho_{eff} = \rho + \rho_{corr} = \rho \left(1 - \frac{\rho}{\rho_{cr}}\right)^\gamma \quad (3.71)$$

again we shall examine the case where $\gamma = 1$ because for $\gamma > 1$, the scale factor $a \rightarrow a_{cr}$ only as $t \rightarrow \infty$. Following the same process as for the quantum inspired dust case, except having the mass now time dependent as $M(t) = M_0/a$, we find

$$\dot{a}^2 = \frac{M_0}{a^2} + \alpha_1 \frac{3M_0^2}{a^6} + \dots, \quad (3.72)$$

and for an effective density of the form $\rho_{eff} = \frac{3M_{eff}}{a^4}$,

$$\dot{a}^2 = \frac{M_0}{a^{4\gamma+2}} (a^4 - a_{cr}^4)^\gamma. \quad (3.73)$$

From the initial condition $a(0) = 1$, with $\gamma = 1$, we find

$$t(a) = \frac{\sqrt{1 - a_{cr}^4} - \sqrt{a^4 - a_{cr}^4}}{2\sqrt{M_0}}. \quad (3.74)$$

We can see that the scale function $a(t)$ reaches a_{cr} in finite time. The effective mass for the system is now given by

$$M_{eff} = \frac{M_0}{a} \left(1 - \frac{\rho}{\rho_{cr}}\right), \quad (3.75)$$

where $M_{eff} \rightarrow 0$ as $t \rightarrow t_{cr}$. The effective pressure of the system can be again evaluated using $p_{eff} = -\frac{M_{eff}}{a^2 \dot{a}}$ giving

$$p_{eff} = \frac{\rho}{3} \left(1 - 5\frac{\rho}{\rho_{cr}}\right), \quad (3.76)$$

showing that once we enter the strong field regime, with $\rho \rightarrow \rho_{cr}$, we have a negative effective pressure on the system. Once the density reaches $\rho_{cr}/5$ the pressure becomes negative, and tends to $-4\rho/3$ at the critical limit.

Rearranging equation (3.74) we find the scale factor to be

$$a(t) = (a_{cr}^4 + (\sqrt{1 - a_{cr}^4} - 2\sqrt{M_0 t})^2)^{1/4}, \quad (3.77)$$

which reaches a minimum at $t_{cr} < t_s$, where \dot{a} vanishes, and the system begins to respond and bounce again before the singularity is ever actually reached. At t_{cr} the effective density is zero, which causes gravity to turn off and the bounce to occur.

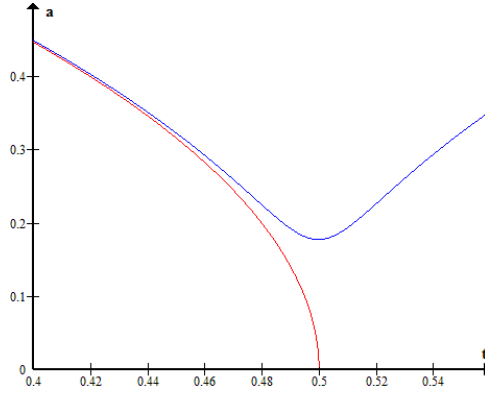


Figure 3.2: **Radiation Scale Factor**

In this graph the red line indicates the scale factor $a(t)$ in the classic case, whereas the blue line represents the quantum corrected model. Initially, in the weak-field regime, the semi-classical model behaves in a similar way to the classical case, however once we get close to t_{cr} , quantum effects become important, and the scale factor diverges from the classical case. We have taken $M_0 = 1$ and $\rho_{cr} = 3000$.

3.3.3 Apparent Horizon

Now we can determine how the trapped surfaces are affected by the bounce process, and whether an event horizon ever fully forms. As stated in the last section, we require $(M_0)r_b^2 < 1$ to ensure no trapped surface forms at the initial time. Semiclassically, this becomes $(M_0)(1 - a_{cr}^4)r_b^2 < 1$.

We find the apparent horizon curve by $a = r^2 M_{eff}$, classically giving us (from equation (3.35))

$$t_{ah}(r) = t_s - \frac{r^2 \sqrt{M_0}}{2}, \quad (3.78)$$

and semi-classically we get

$$r_{ah}(t) = \frac{a^3}{\sqrt{M_0(a^4 - a_{cr}^4)}}. \quad (3.79)$$

Since $t_{ah} < t_s$ there will be an apparent horizon for the collapse process, which will briefly disappear when $a = a_{cr}$ as r_{ah} diverges, and immediately returns until the density of the expanding cloud drops sufficiently.

Once again the apparent horizon curve has a minimum value, given by

$$\frac{dr}{dt} = 0 \Rightarrow a^4 = 3a_{cr}^4, \quad (3.80)$$

$$\Rightarrow t_{min} = t_s(\sqrt{1 - a_{cr}^4} - \sqrt{2}a_{cr}^2), \quad (3.81)$$

where

$$r_{min} = r_{ah}(t_{min}) = 3^{3/4} \frac{a_{cr}}{\sqrt{2M_0}}.$$

If we take the initial boundary $r_b < r_{min}$, no trapped surface can form. Similar to the dust case, if there is a minimum radius this implies there must be a threshold mass below which no apparent horizon can form, given by $2M_T = r_b^3 M_0$,

$$\Rightarrow M_{min} = a_{cr}^3 (3)^{9/4} \sqrt{\frac{1}{32M_0}}. \quad (3.82)$$

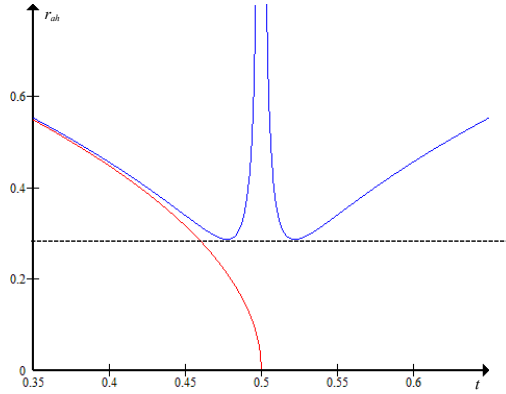


Figure 3.3: Radiation Apparent Horizon Graph

This is a graph of the apparent horizon curve $r_{ah}(t)$ for the classical model (red line) and semiclassical model (blue line). We can clearly see that as $t \rightarrow t_{cr}$, $r_{ah} \rightarrow \infty$, so the process becomes visible to an observer at infinity for a brief period of time.

The penrose diagram would be much the same as for figure (2.3), also having no null geodesics disconnected from future null infinity.

4 Massless Scalar Field Models of Gravitational Collapse

We now move onto the gravitational collapse model of a massless scalar field. The massless scalar field is an interesting model as it has consequences for collapse scenarios as well in cosmology. In cosmology "one would like to know the behaviour of fundamental matter fields towards understanding the transition from matter dominated regime to dark energy domination" [38]. Scalar fields can also act as 'effective' cosmological constant driving an inflationary period of the universe. We examine the dynamic collapse of a scalar field to hopefully gain some insight into phenomena like gravitational collapse or cosmic censorship, and maybe gain a better understanding of the early universe.

I will begin by giving some mathematical background for dealing with scalar fields in spacetime, and then examine the different classes of gravitational collapse models that can come about as a result. We will describe models where the singularity is formed simultaneously as the collapse progresses, and see how the process is changed between homogeneous and inhomogeneous models.

The analysis we shall study is done using comoving coordinates, and such a coordinate system would break if we allowed the gradient of the scalar field to become null, and therefore we only examine the collapse of those models in which the gradient remains timelike throughout the collapse process. Homogeneous and isotropic FRW solutions are examples of this, or scalar fields with inhomogeneous perturbations of a homogeneous background also satisfy this condition.

The requirement that the gradient remains timelike includes a large number of physically relevant collapse scenarios, and is also applicable to the case of dynamic evolution of stiff fluids in a spacetime. This is because a massless scalar field with timelike gradient minimally coupled to gravity has an exact correspondence with a stiff fluid minimally coupled to gravity.

The Lagrangian of a massless scalar field $\phi(x^a)$ in a spacetime (M, g_{ab}) is given by

$$\mathcal{L} = -\frac{1}{2}\phi_{;a}\phi_{;b}g^{ab}, \quad (4.1)$$

and the energy-momentum tensor is

$$T_{ab} = \phi_{;a}\phi_{;b} - \frac{1}{2}g_{ab}(\phi_{;c}\phi_{;d}g^{cd}). \quad (4.2)$$

This massless scalar field is of Type 1, meaning it has one timelike and three spacelike eigenvectors. The eigenvalue ρ gives the energy density, while eigenvalues p_i give the pressure in the three spacelike directions. Choosing comoving spherically symmetric coordinates (t, r, θ, ϕ) , the most general metric is again

$$ds^2 = -e^{2\nu}dt^2 + e^{2\psi}dr^2 + R^2d\Omega^2. \quad (4.3)$$

Generally $\phi = \phi(r, t)$, but since we have a diagonal energy momentum tensor $\phi(r, t) = \phi(r)$ or $\phi(t)$. Since we are interested in the dynamic evolution of the field, we consider $\phi(t)$. In this frame the components are

$$T_t^t = T_r^r = T_\theta^\theta = T_\phi^\phi = \frac{1}{2}e^{-2\nu}\dot{\phi}^2, \quad (4.4)$$

and since

$$\rho(r, t) = p(r, t) = \frac{1}{2}e^{-2\nu}\dot{\phi}^2, \quad (4.5)$$

the field behaves like a stiff fluid with the above equation of state. For a perfect fluid

$$T_{ab} = (\rho + p)u_a u_b + p g_{ab}, \quad (4.6)$$

where the velocity vector is u^μ , and $\rho = p$ for a stiff fluid. Since $\rho_{,\mu}$ is timelike, $\phi_{,\mu}\phi^{,\mu} < 0$, and defining $u_\mu = -\frac{\phi_{,\mu}}{|\phi_{,\mu}\phi^{,\mu}|^{1/2}}$ we re-express the energy momentum tensor for the scalar field as

$$T_{ab} = (|\phi_{,\mu}\phi^{,\mu}|)u_a u_b + \frac{1}{2}g_{ab}(|\phi_{,\mu}\phi^{,\mu}|). \quad (4.7)$$

Denoting $|\phi_{,\mu}\phi^{,\mu}| = \rho = p$, this is the same energy momentum tensor for a stiff fluid.

All energy conditions are then satisfied for real functions $\phi(t)$, and the weak energy condition guarantees that $\phi_{,u}$ is always null or timelike by

$$\begin{aligned} \rho + p &\geq 0, \\ \Rightarrow \dot{\phi}^2 &\geq 0, \\ \phi_\mu \phi_\nu g^{\mu\nu} &= \phi_t \phi_t g^{tt} = -\dot{\phi}^2 e^{-2\nu} \leq 0, \end{aligned}$$

hence we can use a comoving coordinate system without a possible breakdown. For physically reasonable scenarios, the energy density of the field should be expected to increase with time. If we have initially regular conditions where the scalar field gradient is timelike, the density is initially non-zero and will only increase. Clearly throughout the collapse process, the gradient will always remain timelike since $|\phi_\mu \phi^\mu| = 2\rho$.

The Einstein equations for the massless scalar field are given by

$$\rho = \frac{1}{2}e^{-2\nu}\dot{\phi}^2 = \frac{F'}{R^2 R'}, \quad (4.8)$$

$$p = \frac{1}{2}e^{-2\nu}\dot{\phi}^2 = -\frac{\dot{F}}{R^2 \dot{R}}, \quad (4.9)$$

$$\partial_t(R^2 e^{\psi-\nu}\dot{\phi}) = 0, \quad (4.10)$$

$$\dot{G} = 2\frac{\nu'}{R'}\dot{R}G, \quad (4.11)$$

where these all have the usual meanings. Integrating (4.10) we find

$$R^2 e^{\psi-\nu}\dot{\phi} = r^2 f(r), \quad (4.12)$$

with $f(r)$ some function of integration. Eliminating $\dot{\phi}(t)$ from (4.8) and (4.9) gives

$$\frac{F'}{R'} = -\frac{\dot{F}}{\dot{R}} = \frac{1}{2} \frac{r^4 f(r)^2 G}{R^2 R'^2}. \quad (4.13)$$

Given these four Einstein equations with four functions ψ, ν, R, F , solving under the initial data and energy conditions gives the whole evolution for the system. As shown before $G = b(r)e^{2rA}$, and substituting this into the equation above gives

$$2rA(r, a) = \ln \left[\frac{-2M_{,a}a^2(a + ra')^2}{f(r)^2 b(r)} \right]. \quad (4.14)$$

To determine $M(r, a)$ we substitute into the first two parts of (4.13) to get

$$3M + rM_{,r} + Q(r, a)M_{,a} = 0 \text{ where } Q(r, a) = 2ra' + a, \quad (4.15)$$

which have the general solutions $F(X, Y)$ discussed before. Solving this at $r = 0$ to find the boundary conditions gives

$$\lim_{r \rightarrow 0} M(r, a) = \frac{m_0}{a^3}. \quad (4.16)$$

So we an initial regular mass which diverges as $a \rightarrow 0$.

From (4.15) we find

$$a' = W(r, a) = -\frac{3M + rM_{,r} + aM_{,a}}{2rM_{,a}}, \quad (4.17)$$

and using the equation of motion we get

$$\dot{a} = V(r, a) = -e^\nu \sqrt{\frac{M}{a} + \frac{G-1}{r^2}}, \quad (4.18)$$

where the negative sign is taken to describe the collapse. To get a solution of $a(r, t)$, the equation

$$V_{,a}W - VW_{,a} = V_{,r}, \quad (4.19)$$

gives the integrability condition for equations (4.17) and (4.18) [41]. The collapse requires $\frac{M}{a} + \frac{G-1}{r^2} > 0$, which acts as a 'reality condition'. If the condition is not satisfied throughout the process, the system will hit $\dot{a} = 0$ in a finite amount of time and the collapse will become an expansion.

From here we can use the equations of motion to derive the time curve in the same way as for the other models

$$t(r, a) = \int_a^1 \frac{\sqrt{a} da}{\sqrt{B(r, a)}} \quad (4.20)$$

$$\sqrt{B(r, a)} = e^\nu \sqrt{b_0(r)ae^{2rA} + ah(r, \tilde{a}) + M(r, \tilde{a})} \quad (4.21)$$

and the time taken for a shell r to reach $R = 0$, where the spacetime becomes singular, is given by the singularity curve

$$t_s(r) = t(r, 0) = \int_0^1 \frac{\sqrt{a} da}{\sqrt{B(r, a)}} \quad (4.22)$$

For any sufficiently regular $M(r, a)$ we can rewrite this near the center as

$$t_s(r) = t_0 + \chi_1 r + \chi_2 r^2 + \dots \quad (4.23)$$

where $t_0 = t(0, 0)$ is the time at which the central shell becomes singular, and $\chi_i = \frac{1}{i!} \frac{d^i t}{dr^i} |_{r=0}$. As before, χ_1 vanishes because of regularity conditions, so the tangent to the singularity curve is determined by χ_2 in the neighbourhood of the center, which is the term which is responsible for the visibility of the singularity. If $\chi_2 > 0$, we can have outgoing null geodesics from the singularity, and we have a locally naked singularity. If $\chi_2 \leq 0$, the singularity is covered by an event horizon at all times, and we have a black hole.

4.1 Homogeneous Massless Scalar Field Collapse

Classically, the collapse of a homogeneous scalar field will always result in a simultaneous singularity and a black hole, as we will show below. Given that the field is homogeneous, we know $\rho = \rho(t)$. With $\rho = e^{-2\nu}\dot{\phi}^2$, we have $\nu = \nu(t)$, so we can rescale t such that $e^{2\nu} = 1$. The singularity appears when $a = 0$, i.e. when the physical radius goes to zero, so for homogeneous density, $t_s(r)$ is independent of r . In general the time curve is given by

$$t = t_s + h_1(r) = \int_0^1 \frac{\sqrt{a} da}{\left(\frac{a}{r^2}(G-1) + M\right)^{1/2}} + h_1(r) \quad (4.24)$$

where $h_1(r)$ is an arbitrary function. Since t_s is a function of a only, the initial condition $t = t_i \Rightarrow a = 1$ means h_1 must be a constant, and a can only depend on $t \Rightarrow a' = 0$. Equation (4.9) gives us

$$e^{-2\nu}\dot{\phi}^2 = -\frac{2M_{,a}}{a^2} \quad (4.25)$$

implying $M = M(a)$. (4.15) implies $M = \frac{M_0}{a^3}$. If $\nu = \nu(t) \Rightarrow A_{,a} = 0$, so $A = A(r)$. From (4.13)

$$G = -\frac{2a^2 M_{,a}(a + ra')^2}{f(r)^2}, \quad (4.26)$$

and substituting in for M gives $G = \frac{6M_0}{f(r)^2}$. Therefore since $t_s(r) \neq 0$, the integral must have a finite result at $r = 0$. The term in the denominator we need to consider is

$$\frac{1}{r^2}(G-1) = f_1(r), \quad (4.27)$$

where $f_1(0)$ is finite.

$$\Rightarrow f(r)^2 = \frac{6M_0}{1 + f_1(r)r^2}, \quad (4.28)$$

and since $t_s(r)$ is constant, $f_1(r)$ also must be constant. Substituting these values into $G = e^{-2\psi}(R')^2$ above gives

$$e^{2\psi} = \frac{a^2}{1 + cr^2}, \quad (4.29)$$

$$t = - \int \frac{\sqrt{a}}{\left(ca + \frac{M_0}{a^3}\right)^{1/2}} da, \quad (4.30)$$

and the metric becomes the FRW metric

$$ds^2 = dt^2 - a^2 \left(\frac{dr^2}{1 + cr^2} + r^2 d\Omega^2 \right). \quad (4.31)$$

4.1.1 Classic Scalar Field Model

For the flat FRW model, with $c = 0$, we have a collapse model which mirrors the perfect fluid model, except for a stiff fluid with $\rho = p$. From equation (4.30), using the initial condition $a = 1$ at $t = 0$, we find that

$$\Rightarrow a(t) = (1 - 3\sqrt{M_0}t)^{1/3} \quad (4.32)$$

The singularity is reached when $a = 0$, which occurs when $t = t_s = 1/3\sqrt{M_0}$. This model leads us to a simultaneous singularity, with the properties of a fluid as discussed in Section 2.

4.2 Inhomogeneous Massless Scalar Field Collapse

For an inhomogeneous scalar field, the collapse doesn't necessarily end with a simultaneous singularity. Any realistic object that undergoes collapse is sure to have inhomogeneities in its energy density, which is governed by $\rho = \rho(r, t)$. We then apply some reality conditions to make the process more physically reasonable, and examine the resulting collapse model.

These reality conditions are [38]:

1. We must have

$$\lim_{r \rightarrow 0} (ra') = 0.$$

This is because when the condition is violated, a becomes divergent as r goes to zero at the center.

2. Using condition 1 in equation (4.15) gives us $3M + rM_{,r} + aM_{,a} = 0$. Due to the divergences discussed in [38], we must have

$$\lim_{r \rightarrow 0} (rM_{,r}) = 0.$$

This tells us that $\lim_{r \rightarrow 0} M(r, a) = M_0/a^3$ as long as $a \neq 0$, and amounts to saying that

$$M(0, a) = \frac{M_0}{a^3},$$

for all $1 \geq a \geq 0$.

Given these conditions, we can prove some general results about the gravitational collapse of a scalar field, and determine the nature of the singularity. Initially considering the class of solutions with $\dot{a} \leq 0$, the collapse does end in a singularity. If we take $a' \geq 0$ for all $r \geq 0$, we can show that this class of solutions admits no non-simultaneous collapse scenarios. This would imply that the central $r = 0$ shell collapses to the singularity before the outer shells. Requiring these conditions, the scalar field will either collapse to a simultaneous singularity in finite time, or the singularity time $t_s(r)$ diverges along any $r = \text{constant}$ timelike curve.

I will now state some propositions and their conclusions that are elaborated on in [38].

Proposition 4.1 *If $\dot{\phi}(t)$ is divergent at some instant t_1 , there is a simultaneous singularity at $t = t_1$.*

This essentially comes from the fact that $\rho = \frac{1}{2}e^{-2\nu}\dot{\phi}(t)^2$. It follows that if there exists a singularity curve that is not simultaneous, then $\dot{\phi}(t)$ will remain finite.

Proposition 4.2 *If $t_s(r)$ is not constant and if $a' \geq 0$ everywhere in the spacetime, then $t_s(r)$ must be divergent.*

The proof of this, centers around the fact that by using the definition of G in (4.26) in the singularity equation, the denominator of the integrand has to be finite at $r = 0$ or else $t_s(0) = 0$ and the singularity is present from the very beginning, which contradicts the initial data conditions. The finiteness and initial mass conditions give us that $M(r, a)$ is of the form $M(r, a) = \frac{M_0}{a^3} + r^n g(r, a)$ where $n \geq 2$. Since both terms in the denominator are finite as $r \rightarrow 0$, it is shown that we can write the denominator as $\frac{c_1}{a^3}$, where c_1 is some constant.

From equation (4.25) we see that $e^{\nu(0,a)} = \frac{a^3 \dot{\phi}(t)}{\sqrt{6M_0}}$, and can be written as $\lim_{a \rightarrow 0} e^{\nu(0,a)} = a^3 f_3(a)$. So the divergence of t_s will appear when $a \rightarrow 0$, and in the divergent part of the integral

$$t_{sd}(0) = \int_0^\epsilon \frac{\sqrt{a} da}{a^3 f_3(a) (\frac{c_1}{a^3})^{1/2}} = \frac{1}{\sqrt{c_2}} \int_0^\epsilon \frac{1}{a f_3(a)} da \quad (4.33)$$

If the singularity is non-simultaneous, $\dot{\phi}(t)$ is always finite, and $f_3(a)$ is also finite. This gives us a divergent $t_s(0)$. On the other hand, if the singularity is simultaneous, $\dot{\phi}(t)$ is divergent at $a = 0$ by Prop. 1, so $f_3(a)$ also must diverge and we have a finite $t_s(0)$. This shows us that for a massless scalar field, with regular initial data and functions that are at least \mathcal{C}^2 near $r = 0$, if the singularity is non-simultaneous and is increasing in time near the center, then the time taken for the central shell to collapse to the singularity, where $a = 0$, diverges logarithmically. We will now show that for the class of solutions we have been considering, this class of non-simultaneous singular solutions cannot occur.

For any $r = \text{constant}$ curve is timelike, the tangent vector is $\tau = dx^\mu/ds$ has components

$$\tau^\mu = \left(\frac{dx^0}{ds}, 0, 0, 0 \right)$$

Since $ds^2 = e^{2\nu} dt^2$, the proper time along the curve is defined

$$\tau(a(t_f), r) = \int_{a(t_i)}^{a(t_f)} e^\nu dt$$

and $\tau(r, a)$ is the proper time taken for a shell labelled r to reach $a = a(t_f)$, starting from $a = 1$. We define the proper time along the central shell as

$$\tau_0(t) = \int_{t_i}^t e^{\nu(0,t)} dt \quad (4.34)$$

Assuming the time taking to reach the singularity is finite $\Rightarrow \frac{d\tau}{dt} = e^{\nu(0,t)}$.

Proposition 4.3 *If $a' > 0$ at $\tau_0 = \tau_{0s}$, then for any $r_2 > 0$, $\tau_{r_2}(\tau_{0s})$ is divergent.*

This proposition tells us that if $a' > 0$ when the central shell hits the singularity, then the time taken for any other shell to reach the singularity is divergent, therefore any singularity that forms in this class of collapse models must be simultaneous, and a spacelike singularity is the only possibility as the final stage of collapse. Any non-simultaneous singularity will not form in these classes of collapse models.

4.3 Non-Singular Massless Scalar Field Collapse

We next show the possibility of existence of a non-singular class of solutions for our scalar field collapse model [38].

Proposition 4.4 *If there is a solution which satisfies the regularity conditions, and for which $\dot{a} \leq 0$ and $a'(r, t) \geq b$ where $b > 0$, for $r_1 \leq r \leq r_2$ for some $r_1, r_2 > 0$, and $t \in (t_i, \infty)$, then we must have $\tau(a_1, r) > k$ for all $k > 0$ for all r , for some $a_1 > 0$, so the comoving shells never become singular.*

For these solutions, it can be shown that $\dot{a} < l$ and for any $l < 0$ for an infinite interval of coordinate time, implying the collapsing matter would eventually freeze [39].

All classes of solutions satisfying these conditions would be free of singularities. If there are solutions of this type, it would indicate that bouncing models might exist in the framework discussed.

4.3.1 Quantum-Corrected Homogeneous Massless Scalar Field Model

Since there is an exact correspondence between the massless scalar field and a stiff fluid, we can analyse the homogeneous scalar field model bounce model in the same way as a perfect fluid, but with a different equation of state. We once again rewrite Einstein's equations as a classical + corrections, where ρ_{cr} governs the scale at where quantum effects become important. The system has an effective energy density

$$\rho_{eff} = \rho \left(1 - \frac{\rho}{\rho_{cr}} \right)$$

In the case of the scalar field, it is equivalent to a perfect fluid with equation of state $\rho = p$. So from the Einstein equations we find

$$\frac{dM}{da} = -\frac{3M}{a} \quad (4.35)$$

$$\Rightarrow M(t) = \frac{M_0}{a^3} \quad (4.36)$$

Substituting this back into the other density equation we find $\rho = \frac{3M_0}{a^6}$. We get an equation of motion from the equation for the Misner-Sharp mass

$$\begin{aligned} F &= R(1 - G - H) \\ \Rightarrow \dot{R}^2 &= -\frac{r^2 M}{a} \\ \Rightarrow a^4 \dot{a}^2 &= M_0 \end{aligned} \quad (4.37)$$

Combining these equations gives us an equation of motion in terms of real density

$$\dot{a}^2 = \frac{M_0}{a^4} + \frac{1}{\rho_{cr}} \frac{3M_0^2}{a^{10}} + \dots \quad (4.38)$$

$$= \frac{M_0}{a^{10}} (a^6 - a_{cr}^6) \quad (4.39)$$

The effective mass is now given by

$$M_{eff} = \frac{M_0}{a^3} \left(1 - \frac{\rho}{\rho_{cr}} \right) \quad (4.40)$$

which goes to zero as $t \rightarrow t_{cr}$. The effective pressure is still given by

$$p_{eff} = -\frac{\dot{M}_{eff}}{a^2 \dot{a}} = \rho \left(1 - \frac{3\rho}{\rho_{cr}} \right) \quad (4.41)$$

This pressure clearly tends to the original equation of state $p = \rho$ in the weak field limit. Once the quantum effects become important, and the density reaches $\rho_{cr}/3$, the pressure starts to become negative. This continues until the critical point t_{cr} when the quantum effects reverse the gravitational collapse, causing the collapsing object to re-expand again.

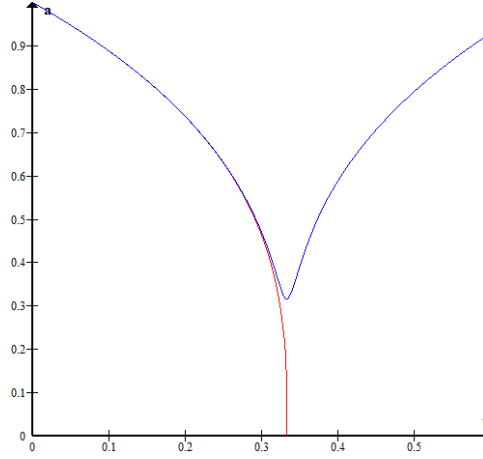


Figure 4.1: **Massless Scalar Field Scale Factor**

In this graph the red line indicates the scale factor $a(t)$ in the classic case, whereas the blue line represents the quantum corrected model. Initially, in the weak-field regime, the semi-classical model behaves in a similar way to the classical case, however once we get close to t_{cr} the quantum effects become important, and the scale factor diverges from the classical case. We have taken $M_0 = 1$ and $\rho_{cr} = 3000$.

Using this equation along with the initial condition that $a(0) = 1$ we find the collapse time curve to be

$$t(a) = \frac{1}{3\sqrt{M_0}} (\sqrt{1 - a_{cr}^6} - \sqrt{a^6 - a_{cr}^6}) \quad (4.42)$$

which can be rearranged to give us the equation for the scale factor

$$a(t) = [a_{cr}^6 + (\sqrt{1 - a_{cr}^6} - 3\sqrt{M_0 t})^2]^{1/6} \quad (4.43)$$

This reaches a minimum at $t_{cr} < t_s$, so the collapse never reaches a singular state. At t_{cr} , $\dot{a}(t_{cr}) = 0$, and from there the object starts to expand again.

4.3.2 Apparent Horizon

The equation for the apparent horizon, $F = R$, becomes

$$r^2 = \frac{a}{M_{eff}} \quad (4.44)$$

$$\Rightarrow r_{ah} = \frac{a^5}{\sqrt{M_0(a^6 - a_{cr}^6)}} \quad (4.45)$$

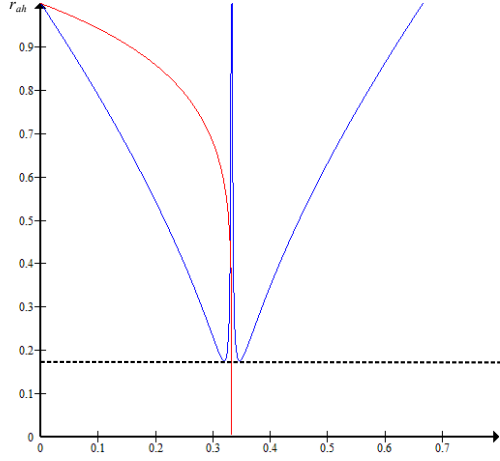


Figure 4.2: **Massless Scalar Field Apparent Horizon Graph**

This is a graph of the apparent horizon curve $r_{ah}(t)$ for the classical model (red line) and semiclassical model (blue line). We can clearly see that as $t \rightarrow t_{cr}$, $r_{ah} \rightarrow \infty$, so the process becomes visible to an observer at infinity for a brief period of time. Unlike the previous cases, there is a large deviation of the r_{ah} curve in the semi-classical case. This is due to the dependence of r_{ah} on M_{eff} , which in turn depends on $1/a^3$.

We can again find the minimum radius r_{min} , below which no apparent horizon can form throughout the whole collapse process. Using $dr/dt = 0 \Rightarrow a^6 = (5/2)a_{cr}^6$, we find it is approached as t tends to

$$t_{min} = t_s(\sqrt{1 - a_{cr}^6} - a_{cr}^3\sqrt{\frac{3}{2}}).$$

From this,

$$r_{min} = r_{ah}(t_{min}) = a_{cr}^2\sqrt{\frac{2}{M_0}}\left(\frac{3}{2}\right)^{5/6}$$

which is the radius such that if the boundary $r_b < r_{min}$, no trapped surfaces will form throughout the collapse. In figure (4.2), it is shown as the black dashed line. This allows us to find the minimum mass for such a process by $2M_T = r_b^3M_0$, hence

$$M_{min} = a_{cr}^6\sqrt{\frac{2}{M_0}}\left(\frac{3}{2}\right)^{15/6} \quad (4.46)$$

In figure (4.2), unlike the previous cases, we see that there is a rather large immediate deviation between the classical and semi-classical apparent horizon curve. In my opinion, this should be expected though, given that $r \propto 1/M_{eff} \Rightarrow r \propto a^2$. This a^2 -dependence of r_{ah} would cause the horizon to drop off much quicker than in the classical case, as a decreases towards the quantum bounce. Again, due to the homogeneous nature of the system, we see that at the bounce point the process is visible to observers at infinity, however this just a result of the homogeneous nature of the system, and in a more realistic scenario the different shell-bouncing times would most likely ensure that the process was surrounded by an apparent horizon at all stages of the collapse, until it disappeared forever.

5 Conclusions

Occam's Razor - *"All things being equal, the simplest solution is usually the correct one."*

In this paper I have examined various models in which I took a gravitationally collapsing object, of a certain matter type, applied a few physically reasonable conditions, and showed that there are many classes of non-singular solutions to these models. I chose to work on these models because I feel that, while a huge amount of work has been focused on black holes, we don't even have proof for the existence of them. Even if we ignore the fact that there is little evidence for real, physical black holes, the problems that come about due to the nature of the singularity are hard to overlook. There are currently many attempts to solve these issues, whether through extra dimensions, the holographic theory, alternate universes, or any number of other ideas, but very few focus on the possibility that a black hole might not actually form, just something that can look like one. This seems like a much more intuitive solution to the black hole problem.

In the models covered, I have shown how the collapse would come about from a general, spherically symmetric metric, and given examples of singular collapse model in each case. These models were examined in the homogeneous and inhomogeneous cases, to determine the nature of the singularity that arises as the end state of collapse. For each of the homogeneous models, the process of collapse ended in a simultaneous singularity, in which all matter shells collapsed to the singularity at the same time, and this collapse was at always covered by an apparent horizon. This resulted in the formation of what we know to be a black hole.

I then went on to examine models of inhomogeneous collapse, where the inhomogeneities were introduced as small perturbations around the homogeneous case. In both the dust and perfect fluid cases, these pressure/density perturbations changed the outcome of collapse rather drastically. In the case of the inhomogeneous dust collapse, a black hole can only form as the result of a simultaneous singularity collapse, and under pressure perturbations the nature of the singularity was determined by one factor, g_{0s} . If this was chosen such that χ_2 was positive, the end state of collapse resulted in a naked singularity. In the inhomogeneous fluid case, once small pressure perturbations were introduced the process had no choice but to end as a naked singularity. Clearly the black hole solution is an extremely unstable one, since small perturbations of the mass profile give us a vastly different outcome.

I then went on to show how by making some slightly different assumptions, the collapse can be halted at a certain point and the object begins to re-expand. This is caused by an as-yet unknown quantum reaction, which halts the collapse and exerts a "force" on the inward-falling matter to counter-act gravity, giving us an effective theory for the collapse. The idea for this semi-classical case comes from some recent results in LQC [1], in which they find the scale factor of the universe to go as

$$\left(\frac{\dot{a}}{a}\right)^2 = \frac{8\pi G}{3}\rho\left(1 - \frac{\rho}{\rho_{cr}}\right), \quad (5.1)$$

The interesting thing about this theory is that the point at which quantum effects become important isn't governed by the Planck length, but rather a Planckian density

$$\rho_{cr} \sim m_p/l_p^3 \sim c^5/(\hbar G^2).$$

Exploiting the analogy between QG effects on black-hole and cosmological singularities, I explain how close to $r = 0$ this quantum "force" will cause a gravitationally collapsing object to expand, resulting in a "quantum bounce".

I have also shown how the apparent horizon for these various cases forms, and give the equation for it in each case. This is important because it governs what an observer at infinity will see throughout the process, and whether we really have a naked singularity or a black hole. In each of the quantum cases the apparent horizon is shown to cover the object for most of the collapse process. The homogeneous models, which are the much simpler cases, have an apparent horizon that disappears momentarily at the point when collapsing object undergoes the "quantum bounce". This is a property of the simultaneous bounce of each of the shells. In the inhomogeneous dust case, we see that each shell will bounce at a different time, meaning the gravity never fully turns off, causing the object to remain covered for the entirety of the process.

An interesting idea I would like to follow-up to this paper, besides examining the quantum-corrected inhomogeneous fluid and scalar field models, is to calculate and compare the proper time for the collapse and bounce to occur with the time taken as seen from an observer at infinity. It should show that for an observer at infinity, the time taken would be of the order of a black hole's lifetime due to the intense gravitational time dilation, however to an observer sitting on the surface of the star the process would happen in a (relatively) much shorter time. As discussed in [1], a Planck star is essentially a shortcut to the distant future, since any observer who managed to land on the surface of the object at some point during the collapse would be bounced with the object through a "very short" proper time to the end stage. This would be extremely far future of the observer at infinity.

This bounce process solves many of the issues surrounding black holes. The non-singular nature of it means that nothing is disconnected from future null infinity, and therefore we have a restoration of unitarity in the spacetime. I think it is the simple nature of this solution that makes it so intriguing. It is a very intuitive idea that a collapsing object would reach a minimum size, governed by the density of the object, and after this point could explode its material outwards again due to some as-yet unknown quantum forces.

This type of theory is also in the realm of somewhat-testable, if we could determine the time a process like this would take for a more physically realistic star that may have formed a primordial Planck Star in the early universe. If one of these primordial Planck Stars were to be coming to the end of its lifetime in this era of the universe, there may be some extremely energetic processes occurring which could be attributed to the end of this process, when the star's boundary emerges from the apparent horizon. While this would still probably be quite a long way off, it does offer some more possibility for testing than alternate universe theories, or physically investigating the interior of a black hole.

References

- [1] C.Rovelli and F. Vidotto, "*Planck Stars*", arXiv:1401.6562 [gr-qc] (2014).
- [2] A.Ashtekar, T.Pawłowski, and P.Singh, "*Loop quantum cosmology of $k=1$ FRW models*", *Physical Review D* **75** 24035 (2007).
- [3] S.B.Giddings, "*Black Holes and Massive Remnants*", arXiv:9203059 [hep-th] (1992).
- [4] S.B.Giddings, "*The black hole information paradox*", arXiv:9508151 [hep-th] (1995).
- [5] S.A.Hayward, "*The disinformation problem for black holes*", arXiv:0504037 [gr-qc] (2005).
- [6] C.Bambi, D.Malafarina, and L.Modesto, "*Terminating black holes in asymptotically free quantum gravity*", arXiv:1306.1668 [gr-qc] (2014).
- [7] D.Malafarina and P.S.Joshi, "*Thermodynamics and gravitational collapse*", arXiv:1106.3734 [gr-qc] 2011.
- [8] S.A.Hayward, "*General laws of black hole dynamics*", arXiv:9303006 [gr-qc] (1994).
- [9] S.A.Hayward, "*Formation and evaporation of non-singular black holes*", arXiv:0506126 [gr-qc] (2005).
- [10] S.K. Rama, "*Remarks on Black Hole Evolution a la Firewalls and Fuzzballs*", arXiv:1211.5645 [hep-th] (2014).
- [11] L.Rezzolla, "*An Introduction to Gravitational Collapse to Black Holes*", (2010).
- [12] W.A.Hiscock, "*Models of evaporating black holes, I*", *Physical Review D* **23**, 2813 (1981).
- [13] W.A.Hiscock, "*Models of evaporating black holes, II*", *Physical Review D* **23**, 2823 (1981).
- [14] P.S.Joshi, "*Gravitational Collapse*", arXiv:9702036 [gr-qc] (1997).
- [15] P.S.Joshi, "*Gravitational Collapse and Spacetime Singularities*", p.210-238 (2007).
- [16] P.S.Joshi and R.Goswami, "*Role of initial data in spherical collapse*", *Physical Review D* **69**, 064027 (2004).
- [17] P.S.Joshi and I.H.Dwivedi, "*Initial data and the end state of spherically symmetric gravitational collapse*", *Classical Quantum Gravity* **16** (1999).
- [18] C.Hellaby and K.Lake, "*Shell Crossings and the Tolman Model*", *Astrophysical Journal* **290** (1985).
- [19] P.S.Joshi, Ravindra V. Saraykar, "*Shell-crossings in Gravitational Collapse*", *International Journal of Modern Physics D* **22** 1350027 (2013).
- [20] R.Goswami and P.S.Joshi, "*Spherical gravitational collapse in N -dimensions*", arXiv:0608136 [gr-qc] (2008).

- [21] S.A.Hayward, "Gravitational energy in spherical symmetry", arXiv:9408002 [gr-qc] (2002).
- [22] D.Malafarina and P.S.Joshi, "Gravitational collapse with tangential pressure", arXiv:1009.2169 [gr-qc] (2011).
- [23] T.P.Singh, "Gravitational Collapse, Black Holes, and Naked Singularities", *Journal of Astrophysics and Astronomy* **20** 221-232 (1999).
- [24] C.Bambi, D.Malafarina, and L.Modesto, "Non-singular quantum-inspired gravitational collapse", arXiv:1305.4790 [gr-qc] (2013).
- [25] P.Joshi and D.Malafarina, "The instability of black hole formation in gravitational collapse", arXiv:1101.2084 [gr-qc] (2011).
- [26] P.S.Joshi and D.Malafarina, "All black holes in Lematre-Tolman-Bondi inhomogeneous dust collapse", arXiv:1405.1146 [gr-qc] (2014).
- [27] Y.Liu, D.Malafarina, L.Modesto, and C.Bambi, "Singularity avoidance in quantum-inspired inhomogeneous dust collapse", arXiv:1405.7249 (2014).
- [28] R.Goswami and P.S.Joshi, "Gravitational collapse of an isentropic perfect fluid with a linear equation of state", *Classical and Quantum Gravity* **21** 3645-3653 (2004).
- [29] P.S.Joshi and R.Goswami, "On trapped surface formation in gravitational collapse", *Classical and Quantum Gravity* **24** 2917-2928 (2007).
- [30] N.O.Santos, "Non-adiabatic radiating collapse", *Monthly Notices of the Royal Astronomical Society* **216** 403-410 (1985).
- [31] A.Banerjee, "Absence of Horizon in the Gravitational Collapse with Radiation", www.imsc.res.in/iagrg/IagrgSite/Activities/.../AsitBanerjee.pdf (2010).
- [32] M.D.Mkenyaleye, R.Goswami, and S.D.Maharaj, "Gravitational collapse of generalised Vaidya spacetime", arXiv:1407.4309 [gr-qc] (2014).
- [33] M.Blau, "Lecture Notes on General Relativity", p.852-878 (2014).
- [34] S.Carroll, "Lecture Notes on General Relativity", p.164-216 (1997).
- [35] P.S.Joshi and R.Goswami, "On trapped surface formation in gravitational collapse II", arXiv:0711.0426 [gr-qc] (2007).
- [36] P.S.Joshi and D.Malafarina, "Instability of black hole formation under small pressure perturbations", arXiv:1105.4336 [gr-qc] (2012).
- [37] S.Satin, D.Malafarina, and P.S.Joshi, "Gravitational Collapse of Inhomogeneous Perfect Fluid", arXiv:1409.0505 [gr-qc] (2014).

- [38] S.Bhattacharya, R.Goswami, and P.S.Joshi, "*Gravitational collapse of a minimally coupled massless scalar field*", arXiv:0807.1985 [gr-qc] (2009).
- [39] S.Bhattacharya, "*Singular and non-singular endstates in massless scalar field collapse*", arXiv:1107.4112 [gr-qc] (2011).
- [40] R.Giambo, "*Gravitational collapse of homogeneous scalar fields*", arXiv:0501013 [gr-qc] (2005).
- [41] R.Goswami, P.S.Joshi, and D.Malafarina, "*Scalar field collapse and cosmic censorship*", arXiv:1202.6218 [gr-qc] (2012).
- [42] Y.Tavakoli, J.Marto, and A.Dapor, "*Semiclassical dynamics of horizons in spherically symmetric collapse*", arXiv:1303.6157 [gr-qc] (2014).
- [43] P.S.Joshi, D.Malafarina, and R.V.Saraykar, "*Genericity aspects in gravitational collapse to black holes and naked singularities*", arXiv:1107.3749 [gr-qc] (2012).
- [44] R.Goswami and P.S.Joshi, "*Cosmic Censorship in Higher Dimensions*", arXiv:0405049 [gr-qc] (2004).